Environmental connotations of benthic foraminiferal assemblages from coastal West Antarctica

Wojciech Majewski[1] *, Julia S. Wellner[2], John B. Anderson[3]

1 Institute of Paleobiology, Polish Academy of Sciences, Twarda 51/55, 00-818 Warszawa, Poland

2 University of Houston, Earth and Atmospheric Sciences, 312 Science and Research Building 1, Houston, TX 77204-5007, USA

3 Rice University, Department of Earth Science, MS 126, PO Box 1892, Houston, TX 77251-1892, USA

* wmaj@twarda.pan.pl

Abstract: This paper examines the variability in foraminiferal assemblages in surface samples from coastal settings along the northwestern Antarctic Peninsula, as well as in the Pine Island Bay area. Material comes from water-depths ranging between 20 and 1257 m, latitudes between 62º and 73ºS, and bottom water temperatures from -1.5 to 1.2 ºC. The microfossil analysis within this broad geographical and environmental context provides a basis of paleo-environmental studies. Environmental affinities of the assemblages were interpreted based on a wide array of ecological conditions, including CTD data, as well as on faunal indices and ecological affinities of the key taxa. Six foraminiferal assemblages are dominated by calcareous taxa. Among other factors, they correspond to variable food supply, terrigenous sedimentation, and water mass properties. Another two assemblages are dominated by arenaceous foraminifera and reflect conditions corrosive to carbonate. Our findings indicate that preserved fossil assemblages in cores from these locations may not be accurate representations of living assemblages.

Keywords: Antarctica, foraminifera, environmental indicators, fjords, CTD.

1. Introduction

Fjord and inland passages are among the best archives of paleoenvironmental records because they (i) are characterized by relatively rapid sedimentation, thus providing good chronostratigraphic resolution, (ii) record processes taking place at the ice-ocean interface, and (iii), they often contain carbonate material for age determination. They were also the last areas of the Antarctic Peninsula (AP) to become free of grounded ice and experience open water conditions (e.g., Shevenell et al., 1996; Milliken et al., 2009; Michalchuk et al., 2009; Allen et al., 2010; Minzoni, in review). Indeed, the current warming trend in the Peninsula has resulted in glacier retreat that may mark the final demise of the remnants of the Antarctic Peninsula Ice Sheet. Future research in this area will focus on the following questions: 1) Is the current warming and associated glacier and ice-shelf retreat in the AP unprecedented or have similar episodes occurred in the past? and 2) What role do other factors, such as the influx or relatively warm ocean waters onto the inner continental shelf and into bays and fjords, play in glacier stability? This current manuscript lays the fundamental groundwork for such future studies by documenting current conditions and how those conditions are recorded in paleo-records.

The aim of this study is to analyze foraminiferal assemblages within bays and fjords from a broad (~2500 km) latitudinal transect, extending from the South Shetland Islands and Antarctic Peninsula to Ferrero Bay in the Amundsen Sea (Fig. 1). Currently, the atmospheric temperature gradient along this transect reaches ~15ºC (Comiso 2000). The region is known to have experienced significant post-LGM climate variability (e.g., Michalchuk et al., 2009; Milliken et al., 2009; Minzoni et al., in press) and is currently one of the most rapidly warming regions on Earth (King et al., 2003; Turner et al., 2005). In addition, the western Antarctic Peninsula region has experienced more intense ocean warming than the global average, more than 1ºC since 1950, as well as increased salinity in the upper 100 meters of the water column (Meredith and King, 2005). This study aims to provide a modern context for

using benthic foraminifera to improve our understanding of climate and environmental change that has occurred since these inland waters first became ice-free. It is part one of a two-part investigation that includes a similar study of diatom assemblages (Swiło et al., in prep.).

Recent, detailed studies of Holocene deposits in the South Shetland Islands and AP fjords have revealed a diachronous record of glacial retreat, which is believed to be due, at least in part, to oceanographic influence, especially warm ocean water masses flowing onto the continental shelf (Michalchuk et al., 2009; Barnard et al., 2014). Detailed foraminiferal assemblage work in the Firth of Tay (Majewski & Anderson, 2009) and Maxwell Bay (Majewski et al., 2012) revealed considerable downcore variability but no unambiguous indication of factors controlling that variability. Thus, there is a need to better understand modern trends in order to place past variability into context.

1.1. Previous foraminiferal studies

To date, foraminiferal research from sediment-surface samples in West Antarctica has been mostly fragmentary and in many cases neglected environmental affinities of different assemblages. This research was initiated in the early 20th century and resulted in key publications that are still used today (e.g., Earland, 1934; see references in Gooday et al., 2014).

In the South Shetland Islands, important works were carried out on foraminiferal re-population of the volcanic caldera of Deception Island by Finger and Lipps (1981) and Gray et al. (2003). Detailed investigations took place around King George Island, including in Admiralty Bay (Majewski, 2005, 2010; Majewski et al., 2007; Rodriguez et al., 2010) as well as in small bays of nearby Maxwell Bay, including Great Wall Bay (all publications in Chinese, see references in Majewski, 2010), Potter Cove (Mayer, 2000), and Marian Cove (Chang and Yoon, 1995). More recent studies followed the retreat of Larsen Ice Shelf aimed

at developing foraminiferal proxies for tracking past ice-shelf collapse (Ishman and Szymcek, 2003; Murray and Pudsey, 2004).

The most comprehensive investigation of the Antarctic Peninsula region was undertaken by Ishman and Domack (1994), who investigated foraminiferal distribution patterns in Marguerite Bay, around the Palmer Archipelago, and in Bransfield Strait. Their research focused on factors controlling benthic foraminiferal distributions which turned out to be the effect of two different water masses; Upper Circumpolar Deep Water and Weddell Sea Transitional Water. Ishman and Domack (1994) did not explore the entire variability of foraminiferal assemblages, especially at locations near shore, and did not discuss their relation with various elements of local environments.

In the Pine Island Bay (PIB) area, early works of Pflum (1966) and Kellogg and Kellogg (1987) addressed only general aspects of foraminiferal distribution and ecology. Later work by Majewski (2013) focused on a relatively limited area of the central PIB and Ferrero Bay and showed a clear trend of decreasing calcareous foraminifera with increasing water-depth. Some of the data presented in that report are incorporated into the present study to analyze them in a much wider context.

1.2. Climatic and oceanographic setting

Coastal areas discussed in this study represent a wide range of Antarctic environments. The most easterly sampling locations are at the northwestern Weddell Sea, which experiences the strongest presence of sea ice, resulting from the Weddell Gyre pushing sea ice towards the AP's east coast (Venegas and Drinkwater, 2001). That area is characterized by a cold continental climate due to the AP acting as a barrier to mild atmospheric and oceanographic conditions extending across Drake Passage (King et al., 2003). Bays and fjords of the eastern tip of the AP are especially influenced by the cold Weddell Sea waters (Fig. 2). They are also characterized by a significant seasonality. In winter, a Winter Mixed Layer develops, i.e.,

isothermal, low salinity water mass with temperatures close to the freezing point. In summer, the upper-most 20-50 m layer of the water column is strongly freshened by meltwater and warmed by solar radiation, leading to formation of Antarctic Surface Waters, below which Winter Waters are present as a remnant of Winter Mixed Layer (Gordon et al., 1984). Because of this stratification, the northwest part of the Weddell Sea, especially the ice-marginal zone, is a region of elevated primary productivity (Kang and Fryxell, 1993; Kang et al., 1995, 2001; Cape et al., 2014).

The South Shetland Islands, located NW across Bransfield Strait from the AP, are the warmest region in Antarctica (King et al., 2003). They are characterized by a relatively warm and humid climate regime with relatively high snowfall and glacial melting and runoff (Reynolds, 1981). Coastal glaciers are characterized by significantly lower altitude of glacial equilibrium lines than elsewhere in Antarctica (King et al., 2003). Due to strong winds and intrusions of relatively warm water masses from Bransfield Strait, winter freezing of the bays is highly variable and quite often they remain free of ice throughout the year (Kruszewski, 2002; Vaughan et al., 2003). The upper water column (to depths of ~ 250 m) of bays is characterized by homogenous temperatures and salinities, implying vertical water mixing (Szafrański and Lipski, 1982; Lipski, 1987). However, during summer a well-defined freshened layer may develop, especially in sheltered bays.

The climate of Graham Land and Palmer Archipelago is colder than that of South Shetlands. The Palmer Archipelago is the region of Antarctica with the greatest precipitation, while Danco Coast, which lies within the precipitation shadow of the Graham Land Plateau, is much dryer (Griffith and Anderson, 1989). The sea-ice distribution shows a strong seasonal pattern, but during summer the area is mostly ice free.

The hydrography of the NW coast of the AP is very complex due to presence and mixing of dense and cold surface water with much warmer and fresher water from the Bellingshausen Sea and Circumpolar Deep Waters (CDW) (Hoffman and Klinck, 1998;

Barcena et al., 2006), (Figs. 1 and 2). Between Palmer Archipelago and Marguerite Bay, waters are influenced predominantly by the Bellingshausen Sea component (Hofmann et al., 1996; Hoffman and Klinck, 1998). This complicated oceanography causes significant variability in physical and chemical parameters along the west AP coast. Coastal waters are characterized by relatively low temperatures and salinities caused by the inflow of glacier and sea-ice meltwater (Garibotti et al., 2003). Intrusions of Lower CDW, which is characterized by high salinity, are generally absent on the Antarctic shelf, but Upper CDW, which is characterized by varying temperature and high nutrient concentrations, does intrude onto the shelf (Orsi et al., 1995; Ducklow et al., 2007), bringing warm, salty water to the shelf. Within fjords, oceanographic circulation is dominated by mid- and deep-water, cold-water tongues generated by glaciers, intrusions of deep and saline waters from open sea, and warm and freshened surface layer development during the summer (Domack and Ishman, 1993). Decreasing influence of melt water in an offshore direction results in warmer, more saline water masses. Relatively high nutrient concentrations throughout the area allows for high phytoplankton productivity (Garibotti et al., 2003).

The most polar sampling area is PIB, located in the Amundsen Sea (Fig. 1). Coastal areas in PIB experience high precipitation rates, especially during winter, due to synoptic-scale cyclones traveling around the Antarctic that come ashore in this region (Vaughan et al., 2001). At water depths below ~300 m, PIB is influenced by the intrusion of relatively warm CDW, with salinities >34.6 ppt and temperatures ~ 3.5º C above the freezing point. This warm water flows onto the inner continental shelf and melts the underside of the ice shelf, thus posing considerable threat to the stability of Pine Island Glacier (Jacobs et al., 2011, 2012). PIB is one of the largest drainage outlets for the West Antarctic Ice Sheet, and because of its unstable ice sheet configuration has been called the "weak underbelly" of the West Antarctic Ice Sheet (Hughes, 1981). The Amundsen

and Bellingshausen seas have both experienced decreasing sea-ice during recent decades (Parkinson and Cavalieri, 2012).2. Material and methods

The 34 samples used in this study come from West Antarctic coastal sites of South Shetlands, the AP, and PIB area (Fig. 1). Except the sample from KC 1A taken from 2.5-4.5 cm interval, most samples are from the uppermost 2 cm of Kasten cores collected during three *RV/IB Nathaniel B. Palmer* cruises: NBP0502, NBP0602A, and NBP0703 between 2005 and 2007 and a single *R/V Oden* cruise OSO0910 from 2010 (Table 1). Four samples from Admiralty Bay, King George Island, were collected in early 2007 using Van Veen and Kajak samplers and represent the true sediment-water interface. Only the Admiralty Bay samples, and those from the PIB area were treated for foraminiferal analysis shortly after recovery. Samples from cores recovered during the *Palmer* cruises were obtained from the core repository at the Antarctic Research Facility at the Florida State University. The same samples used for foraminiferal analysis were also analyzed for diatoms. Results of the later investigation are presented in Świło et al. (in prep). Water temperature and salinity data were collected using a CTD profilers during the NBP0703 and Oden cruises. Processing of the CTD data was completed using Sea-Bird Electronics data processing software.

2.1. Sample treatment

Samples were wet-sieved with tap water through a 63 μm sieve and dried. Foraminifera were picked from >63 μm fraction. Although analyzing minute foraminifera may potentially increase dissolution bias in assemblages as it is shown later, minute species are frequently the most distinctive elements of assemblages. In 20 samples, all foraminiferal specimens were picked. Thirteen samples yielding large numbers of foraminifera were divided using a dry microsplitter and a fraction of residue was analyzed. No less than 250 specimens were picked from each of the foram-rich samples. All foraminiferal specimens were arranged by taxa on micropaleontological slides. The investigated material is housed at

183 the Institute of Paleobiology of the Polish Academy of Sciences (Warszawa) under the
184 catalogue number ZPAL F.65. From the residues processed for foraminifera, weights of dry
185 sample fractions finer than 63 μm, between 63 and 500 μm, and coarser than 0.5 mm were
186 noted. These crude data were used only as a granulometry background for
187 micropaleontological analyses (Appendix 1).
188
189 **2.2. Foraminiferal taxonomy**
190 The classification scheme for the Order Foraminiferida used here is that of Loeblich
191 and Tappan (1987). Species identification followed Majewski (2005, 2010, 2013) and
192 Majewski et al. (2007). Distinction between *Globocassidulina biora* and *Globocassidulina*
193 *subglobosa*, especially among minute specimens, is problematic (e.g., Majewski and
194 Pawlowski, 2010). In this study, individuals of *G. biora* were identified based on slightly
195 compressed tests and any signs of bifurcation or bending of the aperture, as well as by a
196 markedly inclined aperture in relation to the last suture. *Globocassidulina subglobosa* was
197 represented by rather minute forms with a straight aperture perpendicular to the last suture.
198 Because of the very problematic discrimination of *Portatrochammina bipolaris*,
199 *Portatrochammina antarctica* and *Portatrochammina bullata*, especially among minute
200 specimens, they are all quantified as *Portatrochammina* spp.
201
202 **2.3. Dataset analyses**
203 For quantifying benthic foraminiferal assemblage diversities, for each sample, the
204 Shannon diversity index (H) was calculated using the following equation $H = -\Sigma\, n_i/n \ln (n_i/n)$,
205 where n_i is the number of individuals of species i. Foraminiferal plankton-to-benthos ratio was
206 calculated as p/b ratio = $p/(p+b)$, where p indicates the number of planktonic and b the
207 number of benthic forms.

To improve understanding of the assemblages investigated in this study, the foraminiferal frequencies were analyzed with orthogonal rotated (Varimax) principal component (PC) analysis, according to Malmgren and Haq (1982) and Mackensen et al. (1990) with a commercially distributed statistics package SYSTAT 12. This procedure was chosen to reduce the number of variables to a manageable number without a significant loss of information. Species that comprised less than 2% of the total assemblages in a single sample were not included, as they are not present in sufficient abundance to be significant statistically. This procedure left 39 taxa for statistical treatment.

The calculated PC scores show the contribution of the selected variables, i.e., foraminiferal species for each PC. Taxa that favor similar environmental conditions are expected to have high scores on one PC, indicating their presence in one assemblage. PC loadings show similarities between assemblages from different sites. Those exceeding a value of 0.4 are regarded as statistically significant, following Malmgren and Haq (1982). At a single site, more than one PC may show values above the significance level, suggesting an intermediate type of assemblage.

3. Results

3.1. CTD data

Detailed information about water mass properties and circulation within AP bays is quite sparse, so we attempted to acquire CTD profiles on an opportunistic basis (Fig. 2). While these data are limited, they show considerable variability in water mass structure between bays, especially in bays on the western side of the AP and at water depths below ~250 m. This reflects their variable bathymetry and connectivity to major ocean currents flowing along the continental margin and within deep inland passages.

The coldest waters (average ~ -1.6°C) occur in Hope Bay, a shallow fjord on the Weddell Sea side of the AP. Salinity is constant (~34.2 ppt) below the surface layer to a water

depth of 126 m (Fig. 2). This is consistent with cold, relatively fresh Weddell Sea Transitional Water that flows northwards along the eastern side of the Antarctic Peninsula (Hofmann et al., 1996; Martinson et al., 2008), (Fig. 1).

The Maxwell Bay water column exhibits constant temperature and salinity to a depth of 250 m, below which the water is colder and slightly more saline (Fig. 2). The presence of a cold bottom layer was an unexpected outcome and implies that cold Weddell Sea waters may be entering the bay from Bransfield Strait at depths below ~ 300 m. This is in contrast to the water column profile from Lapeyrère Bay, which is the deepest fjord sampled along the western side of the AP. The CTD profile from Lapeyrère Bay shows salinity and temperature increasing throughout the 625 thick water column, with temperatures greater than 1.0°C in the lower 100 m (Fig. 2). The bay is located within Anvers Island and connected to the open shelf via a v-shaped trough (Fig. 1). Thus, it is more subject to incursion of warm deep water that flows north along the continental margin.

Both Paradise Harbor and Collins Bay are shallow fjords located on the western side of the AP. A CTD collected in front of Miethe Glacier in Paradise Harbor shows relatively constant temperature and salinity with depth. Nearby in Collins Bay, a CTD profile collected just 200 m from the glacier terminus where a sediment-rich meltwater plume was observed, revealed fresher, colder water near the surface, with a gradual increase in both temperature and salinity with depth in the water column. Relatively warm water (0.7°C) was measured just below 200 meters water depth (Fig. 2), suggesting possible influence from warm impinging currents.

The CTD data from Ferrero Bay and central Pine Island Bay show some of the warmest water observed (>1.0°C; Fig. 2) in this data set, consistent with observations of Jacobs et al. (2011, 2012) of CDW intrusion onto the continental shelf. The 2010 Oden CTD profile shows that this warm water extends into Ferrero Bay (Fig. 2).

3.2. Foraminiferal data

A total of 49 benthic foraminiferal species were quantified and listed on Appendix 1. They are accompanied by a low number of specimens belonging to unidentified species reported as "other" agglutinated and calcareous benthic foraminifera as well as by a few planktonic *Neogloboquadrina pachyderma*. Plankton-to-benthos ratios at most sites are nearly 0; only at three locations it exceeded 0.1 (Fig. 3). The diversity index *H*, calculated for the census data presented in Appendix 1, shows values between 0.5 and almost 2.9, suggesting a weak overall trend of increasing *H* with increasing water depth (Fig. 4). Agglutinated forms are represented by 29 species, and calcareous by 20 species. Percent of calcareous foraminifera ranges broadly between 0 and 100%, showing the highest values in the South Shetlands and the lowest in the NW Weddell Sea sites (Fig. 4). The most abundant species that average over 5% of all specimens are *Globocassidulina biora* and *Portatrochammina* spp. (11% each), *Epistominella* spp. and *Astrononion echolsi* (both ~ 8%), and *Fursenkoina fusiformis*, *Globocassidulina subglobosa*, and *Miliammina arenacea* (all well over 5%). They all contribute strongly to the assemblages identified in the foraminiferal PC analysis, therefore their distribution is well reflected by foraminiferal assemblages discussed later.

The proposed eight-PC model explains 85.7% of the total variance of the data set (Tables 2 and 3). Seven PCs are defined by a single species with PC scores well over 5.0 that may be accompanied by accessory species with elevated (> 1.0) PC scores. One PC is defined by three species, showing scores between 2.2 and 3.7. For clarity in the upcoming discussion, the calculated PCs, which are mathematical models of real assemblages, are referred to as foraminiferal assemblages (FAs) using the names of the taxon of the highest PC score. The eight PCs are (1) the *Portatrochammina* spp. FA (15.9 % of total variance explained, with accessory *Adercotryma glomerata*), (2) the *Epistominella* spp. FA (13.9 % with no accessory species), (3) the *Globocassidulina biora* FA (13.7 %, with accessory *G. subglobosa*), (4) the *Astrononion echolsi* FA (11.6 % with accessory *S. biformis*), (5) the *Bolivinellina*

286 *pseudopunctata* FA (10.6 % with no accessory species), (6) the *Fursenkoina fusiformis* FA
287 (8.6 %, with accessory *M. arenacea* and *G. subglobosa*), (7) the *Miliammina arenacea* FA
288 (6.9 %, with similarly high scores of *S. biformis* and *P. bartrami*) and finally (8) the *Bulimina*
289 *aculeata* FA, explaining 4.5% of the total variance of dataset and with *S. biformis* showing
290 high PC scores of opposite sign.
291 Distribution of sites with high PC loadings for each FA is shown on Fig. 1. The *G.*
292 *biora* FA dominates most sites on King George Island along with three other locations
293 throughout the NW shores of the AP, while the *B. pseudopunctata* FA occurs only in outer
294 Admiralty and Maxwell bays as well as at a single site within Flandres Bay. The *F. fusiformis*
295 FA and the *A. echolsi* FA are prominent at several sites throughout coastal waters of Graham
296 Land, and the *B. aculeata* FA at a single site KC 49 off Beascochea Bay. The *Epistominella*
297 spp. FA is dominant only at sites in central PIB. The *Portatrochammina* spp. FA is dominant
298 in the NW Weddell Sea and a few sites in the PIB area, and finally the *M. arenacea* FA is
299 dominant mostly in Gerlache Strait between Palmer Archipelago and Graham Land.
300
301 **4. Discussion**
302 **4.1. Evaluation of foraminiferal data**
303 Earlier studies in Admiralty Bay (Majewski, 2005; Majewski et al., 2007) and PIB
304 (Majewski, 2013) support a general observation that the environmental conditions affecting
305 benthic foraminiferal assemblages commonly change with bathymetry (e.g., Gooday et al.,
306 2014). Frequently, the water depth is also the most precise characteristic of sampling sites,
307 which is especially true in the case of predominantly subfossil assemblages. Therefore, for
308 analyzing different foraminiferal indices, plotting them against water-depth (Figs. 3-5) is the
309 most effective way to analyze their relationship to other variables.
310 It is important to keep in mind that there are significant differences between sites
311 discussed in this study in coring and sampling methods as well as in time lag between

312 sediment recovery and sample processing. Moreover, Kasten coring, used at the sites
313 investigated during the *Palmer* and *Oden* cruises, may fail to capture the upper-most sediment
314 section so these sites may reflect slightly pre-Modern time slices (see also Majewski, 2013);
315 ^{210}Pb dating from many of the Kasten cores suggests that very little time may be missing
316 (Boldt et al., 2013) . The four samples from Admiralty Bay represent a true sediment-water
317 interface corresponding with the time of sampling, which was 2007.
318 Not accounting for bioturbation, the 2 cm thick slices of the sediment represent
319 averaged records of anywhere between a few and tens of years, depending on sediment
320 accumulation rates which may vary significantly between different locations and within a
321 single section, especially if positioned near-shore (e.g., Griffith and Anderson, 1989; Boldt et
322 al., 2013). For example, in core NPB0703-JTC-17 from Maxwell Bay, the time represented
323 by 2 cm of sediment, based on ^{210}Pb analysis (Majewski et al., 2012), varies between just over
324 a year to almost 60 years. Because precise accumulation rates are not known, interpretation of
325 any absolute data should be treated with caution. In contrast, relative data, e.g., species
326 percentages, do not carry this potential flaw. Given these constraints, our data do not
327 necessarily reflect "living" foraminiferal assemblages, but they do represent Modern
328 assemblages. Therefore, the present day oceanographic conditions (Fig. 2) may provide only a
329 general background for interpretation of our micropaleontological data.
330 The potentially sub-fossil nature of our datasets results not only in weaknesses but also
331 in important advantages. The microfossil assemblages discussed in this study are much closer
332 in taxonomic composition to assemblages used for paleoenvironmental reconstructions than
333 "living" foraminiferal assemblages investigated by many workers (e.g., Finger and Lipps,
334 1982; Ishman and Domack, 1994; Majewski, 2005). This is especially true for samples with a
335 large proportion of agglutinated foraminifera that tend to disintegrate downcore (e.g.,
336 Majewski and Anderson, 2009). Therefore, their present analysis is of more practical value
337 for interpreting young geological records.

4.2. Low plankton-to-benthos ratios in coastal West Antarctica

Zero to very low numbers of planktonic foraminifera collected at most sites seem to reflect most of all near-shore locations of these sites, where sediment laden and freshened surface waters result from glacier melting and runoff. At deeper-water settings, in areas of high productivity, and CDW presence, dissolution may be also an issue. Thus, it is not surprising that the only p/b values substantially higher than zero are from PIB (Fig. 3), apparently representing the most open water conditions among our sites. Moreover, as for other faunal characteristics, the p/b ratios from the PIB sites show a clear trend of rapidly declining below ~700 m water depth (see also Majewski, 2013), reflecting increasing dissolution due to stronger CDW presence.

4.3. Benthic foraminiferal diversities

Although *H* values shows a pattern of increasing values with increasing water-depths, only in the PIB area is this trend well defined (Fig. 4). It is apparent, however, that the *F. fusiformis* FA, and to a lesser degree the *A. echolsi*, *M. arenacea*, and *B. pseudopunctata* Fas, show rather high and elevated *H* values, while the *G. biora* FA has the lowest *H*. Among our samples. The general pattern, although obscured by other factors, is that the lowest faunal diversities are reported from shallow water, near-shore, and restricted environments while the highest *H* values are typical for more open marine, deeper water habitats that are assumed to experience less extreme environmental variability.

The important exceptions from this general trend (e.g., KC 8A, KC 29 and KC 49 from Firth of Tay, Flandres Bay, and off Beascochea Bay, respectively) show significantly impoverished *H* values, which may result from post-depositional processes, such as dissolution that could selectively remove a group of less robust taxa from the sub-fossil record. On the contrary, at sites KG 13 and KC 14 from King George Island, the *H* values seem to be rather higher than might be expected. This inconsistency could be explained by

364 faunal mixing, which might be supported by foraminiferal assemblages that in both cases are
365 poorly explained by the PC analysis, or by higher sedimentation rates and lower organic
366 content indicating less corrosive conditions.
367
368 **4.4. Percentages of calcareous benthic foraminifera**
369 Patterns within the plot of percent calcareous benthic foraminifera against water-depth
370 (Fig. 5) are especially intriguing. First of all, a clear distinction between the four sampling
371 areas is apparent. As for the other indices, the best defined trend is exhibited by the samples
372 from the PIB area, showing a clear decline in the percentage of calcareous forms with depth
373 between ~600-800 mwd. Only sample KC 16 does not follow this trend, which could to be
374 due to the presumed markedly older age of this sample as compared to other samples from
375 PIB (see also discussion in Majewski, 2013).
376 In general, samples from Admiralty and Maxwell bays show the highest percentages
377 of calcareous forms. Even in sample KC 1A, taken from 488 mwd, calcareous foraminifera
378 constitute 75% of the assemblage. However, sites from Admiralty Bay that were sampled in
379 an earlier survey (Majewski, 2005) at water depths of ~500 m are characterized by relatively
380 low proportions of calcareous forms, between 40% and 15% (Fig. 3). At sites from
381 northwestern Weddell Sea, the percentages of calcareous forms are significantly lower than in
382 the other areas. Instead, assemblages are strongly dominated by agglutinated forms, possibly
383 due to conditions unfavorable for carbonate preservation, which are common throughout the
384 Weddell Sea (Anderson, 1975b; Mackensen et al., 1990).
385 By far the greatest variability in percentage of calcareous forms versus water-depth is
386 exhibited in sites from offshore Graham Land and Anvers Island. Most of these sites,
387 regardless of bathymetry, show values well above 60%. At all sites dominated by the *M.*
388 *arenacea* FA (KC 65, KC 31, and KC 55), percentages of calcareous forms are markedly

lower, between values 30 and 0, while both sites with significant the *B. aculeata* FA (KC 34 and KC 49) show the percentages of calcareous forms being much higher than in PIB (Fig. 5).

4.5. Foraminiferal assemblages

The eight FAs recognized in this work reflect large variability in foraminiferal assemblages and associated environmental conditions. The proposed PC model explains 85.7% of the total variance of the benthic foraminiferal dataset. A weakness in the model is demonstrated by failing to account for site KG 14 by the proposed FAs. The ten-PC model, explaining 91.2% of the total variance, solves this problem, but the additional FAs generated within that model add complexity that hinders straightforward interpretation.

The interpretation of the proposed FAs is presented below according to their environmental affinities. The first six FAs are dominated by calcareous taxa, and arranged more or less according to decreasing glacial influence. The last two FAs, dominated by arenaceous taxa, indicate corrosive conditions. The names of the FAs are indicative of the strongest presence, expressed by the highest PC scores, of the index taxa in particular foraminiferal assemblages (Table 2). Typically the distribution of particular FAs closely follows the geographic distribution of index taxa.

4.5.1. *Globocassidulina biora* FA

The *G. biora* FA shows elevated PC scores of *G. subglobosa* (Table 2) and a significant correlation with *P. fusca* and *Quinqueloculina* sp. (Table 4). This FA tends to be characterized by rather low *H* values (Fig. 4) and high percentages of calcareous foraminifera (Fig. 5). The *Globocassidulina biora* FA dominates at most sites in Maxwell and Admiralty bays, as well as at three other locations along the northwestern coast of the AP (Fig. 1). In Maxwell and Admiralty bays, *G. biora* along with *P. fusca* and *Quinqueloculina* sp. dominate assemblages at less than 200 m and has been shown to indicate strong glacial influence (Li et

al., 2000; Majewski, 2005, 2010; Majewski et al., 2012). Sites KC 48 (Beascochea Bay), KC 63 (Brialmont Cove), and to a less extent KC 57 (Andvord Bay) from the western AP sector (Fig. 1) also yielded high scores of the *G. biora* FA (Table 3). These sites occur in inner bay locations but in considerably deeper water than the Maxwell Bay and Admiralty Bay sites. These locations are all consistent with greater glacier influence, which includes freshwater influx and high sedimentation rates (Majewski et al., 2012; Boldt et al., 2013). Bathymetry does not appear to be a critical factor for dominance of the *G. biora* FA.

In the light of other FAs occupying central and outer fjords that are discussed below, the *G. biora* FA seems to be largely depleted in typical opportunistic species that can feed on intense but short lasting phytodetritus, e.g. *F. fusiformis* and *Epistominella exigua* (Gooday 1993). The relatively high modern sediment accumulation rates at these sites tend to dilute organic flux to the sea floor. The strong glacial influence may also impact primary production by elevated water turbidity, limiting thickness of the photic zone during spring and summer on one hand along with delivery of terrigenous nutrients on the other. The fact that *G. biora* FA also tends to occur at sites far within fjords further implies that this FA should be tolerant to prolonged winter sea-ice conditions that can develop during some years.

4.5.2. *Bolivinellina pseudopunctata* FA

The *B. pseudopunctata* FA is characterized by relatively low PC scores and insignificant correlation coefficients with any other species. This FA is prominent only within fjords in outer Admiralty and Maxwell bays and at a single site (KC 29) within Flanders Bay (Fig. 1). It lacks planktonic foraminifera but otherwise has a high percentage of calcareous species (Fig. 5). The diversity index *H* ranges within intermediate values for this FA (Fig. 4).

In Admiralty Bay, the *B. pseudopunctata* FA corresponds with more sandy sediments (Appendix 2) that are associated with the glacier-proximal *G. biora* FA; it also occurs in greater water depths. This FA is also present in central Maxwell Bay (KC 1A), which at water

441 depth ~500 mwd is affected by cold Weddell Sea waters, as shown by our CTD data (Fig. 2).
442 The *B. pseudopunctata* FA does not seem to be indicative of these cold water masses, as it is
443 also prominent within Flanders Bay, which is under influence of much warmer CDW.
444 Although the *B. pseudopunctata* FA is noted in Flanders Bay, it is also absent in neighboring
445 Andvord Bay. Flanders Bay has a wide mouth connecting it with the open ocean, in contrast
446 to Andvord Bay which has a more narrow mouth and connects to an inland passage, Gerlache
447 Strait. Therefore, Flanders Bay is believed to experience greater marine influence, including
448 stronger circulation and winnowing of finer sediment.
449 The minute size and thin transparent wall of *B. pseudopunctata* may suggest an
450 opportunistic nature and a capacity for rapid growth and reproduction, similarly as *E. exigua*
451 and *Fursenkoina* sp. (Gooday, 1993). In this respect, the *B. pseudopunctata* FA could be
452 similar to the *F. fusiformis* FA, which is prominent in several fjords of the northwestern AP.
453 In addition, a 4-PC model, although not employed in our interpretation, indicates that these
454 two FAs share similar affinities, together with *A. echolsi*, which is abundant in outer
455 Admiralty Bay (Majewski, 2005).
456
457 **4.5.3. *Fursenkoina fusiformis* FA**
458 The *F. fusiformis* FA shows elevated PC positive scores for *M. arenacea* and *G.*
459 *subglobosa* (Table 2), but no significant correlation coefficient with any taxa analyzed. This
460 FA is prominent in several fjords throughout Graham Land and Anvers Island (Fig. 1). It
461 shows rather high percentages of calcareous species (except at site KC 45) as well as high *H*
462 values (Figs. 5 and 4, respectively).
463 The association of *F. fusiformis* with *G. subglobosa*, at sites dominated by the *F.*
464 *fusiformis* FA within deep fjords (~500 m and deeper), is similar to the *Globocassidulina*
465 spp.– F. *fusiformis* assemblage of the Firth of Tay (Majewski and Anderson, 2009). There, it
466 represents the most glacier-proximal conditions. The latter assemblage is accompanied by

467 *Cribroelphidium webbi,* a unique glacier-proximal indicator (Majewski and Tatur, 2009),
468 which is interpreted to thrive during elevated glacier sedimentation and good preservation of
469 carbonate.

470 Ishman and Domack (1994) associated their *Fursenkoina* spp. assemblage, which is
471 prominent throughout Bransfield Strait and the Palmer Archipelago, with Weddell Sea
472 Transitional Water. However, *Fursenkoina* sp. and *G. subglobosa*, both present in our FA,
473 have been suggested to be opportunistic species (*e.g.*, Alve, 1994) and associated with
474 seasonal delivery of phytodetritus to the sea floor (Gooday, 1993). Sen Gupta and Machain-
475 Castillo (1993) noted high tolerance of *F. fusiformis* to organic-rich oxygen-depleted waters.
476 Following these arguments, Ishman and Sperling (2002) interpreted an assemblage dominated
477 by *F. fusiformis* from the lower portion of the Palmer Deep as an opportunistic assemblage
478 favored by intense diatom blooms and episodes of high terrigenous sedimentation. This is
479 consistent with our interpretation.

480

481 **4.5.4. *Astrononion echolsi* FA**

482 The *A. echolsi* FA shows elevated PC scores of *S. biformis* (Table 2) and a significant
483 positive correlation coefficient with *Bolivinellina earlandii* and *Stainforthia concava* (Table
484 4). This FA is prominent at several sites along the Graham Land Coast at locations between
485 those dominated by the most open-water *B. aculeata* FA and the most near-shore *G. biora* FA
486 (Fig. 1). At sites dominated by *A. echolsi* FA, percentages of calcareous species and
487 diversities tend to reach rather high values (Fig. 5).

488 As compared with *G. biora*, *A. echolsi,* together with *B. earlandii* and *S. concava* are
489 considered glacier-distal taxa (Majewski, 2005, 2010). *Astrononion echolsi*, being the most
490 important species for this FA, builds thick-walled, medium-size tests, unlike most
491 opportunistic species (Gooday, 1993). No apparent difference in sediment granulometry is
492 noted between sites dominated by the *A. echolsi* and *F. fusiformis* FAs (Appendix 2), all are

493 fine grained with very little sand. The *A. echolsi* FA is typical for areas with less intense
494 phytodetritus events than the *F. fusiformis* FA. *Astrononion echolsi* is also common in
495 Admiralty Bay (Majewski, 2005), where the sediments are less organic-rich than sediments
496 that have accumulated in bays and fjords along the Danco Coast and along Anvers Island.
497
498 **4.5.5. *Bulimina aculeata* FA**
499 The *B. aculeata* FA shows elevated negative PC scores of *S. biformis* (Table 2) and a
500 significant positive correlation coefficient with *Pullenia sphaerica* (Table 4). This FA
501 dominates at a single site KC 49 off Beascochea Bay, but is also prominent at site KC 34, at
502 the mouth of Laperère Bay (Fig. 1). The location of the later, as well as slightly elevated p/b
503 ratio at KC 49 (Fig. 3), suggests an open-water affinity for this FA. It shows intermediate *H*
504 values (Fig. 4) and relatively high percentages of calcareous forms (Fig. 5), significantly
505 above the trend of assemblages from PIB. This suggests a correlation of the *B. aculeata* FA
506 with oceanographic conditions different from those that characterize the *Epistominella* spp.
507 FA.
508 In the Weddell Sea, *B. aculeata* appears to be associated with organic-rich sediment
509 and warm (> 0ºC) moderately oxygenated waters (Mackensen et al., 1990). According to
510 Ishman and Domack (1994), it is the key species associated with relatively warm CDW
511 impinging onto the AP continental shelf. They also recognized *P. sphaerica*, which is also an
512 important species in our FA, as an important species of their *B. aculeata* assemblage. In our
513 study, the *B. aculeata* FA is restricted to two sites with the highest percentages of this index
514 species. These sites are located farthest offshore and are potentially the most exposed to
515 CDW.
516 Although this work has shown only limited presence of this FA (Fig. 1), it does
517 confirm the presence of individuals of this species in Pine Island Bay, in the southern fjords
518 of the Graham Land Coast, and near Anvers Island, but not in the South Shetland Islands or in

519 the northwestern Weddell Sea sample sites (Fig. 6). The distribution of *B. aculeata*
520 individuals correlates well with areas where warm water was detected in CTDs collected near
521 the sample sites (Fig. 2) and supports the presence of deep water-mass boundary stretched
522 between Anvers Island and Graham Land (Ishman and Domack, 1994; Shevenell and
523 Kennett, 2002), (Fig. 6).
524
525 **4.5.6. *Epistominella* spp. FA**
526 This FA shows a significant positive correlation coefficient with agglutinated
527 (*Rhabdammina* spp., *Adercotryma glomerata*, *Pseudobolivina antarctia*, and *Alterammina*
528 *alterans)*, as well as calcareous species (*Angulogerina earlandi*, *Nonionella iridea*, and
529 *Ioanella tumidula)* (Table 4). This FA is dominant only at sites in central PIB, suggesting its
530 open-water affinity, which is also supported by the highest p/b ratios at sites dominated by
531 this FA (Fig. 3). It is also a minor FA at KC 1A in outer Maxwell Bay. At the sites in PIB, a
532 clear trend of decreasing percentage of calcareous foraminifera and increasing diversity index
533 *H* with increasing bathymetry is apparent (Figs. 5 and 4, respectively).
534 At greater water depths in the PIB area, the *Epistominella* spp. FA is replaced by the
535 *Portatrochammina* spp. FA, which reflects increasing carbonate dissolution and association
536 with corrosive water masses, in this case CDW (Majewski, 2013). The *Epistominella* spp. FA
537 appears to be associated with minimal CDW influence. Two calcareous species associated
538 with the *Epistominella* spp. FA (i.e. *N. iridea* and *I. tumidula)* are known for surrounding
539 their tests with cocoon-like sediment capsules (Mackensen et al., 1990; Murray and Pudsey,
540 2004) that can protect them from outside conditions. This feature, together with
541 accompanying agglutinated species, supports the affinity of this FA with occasionally
542 corrosive conditions. *E. exigua*, which dominates this FA, is also known to be resistant to
543 dissolution (Anderson, 1975a; Ishman and Szymcek, 2003).

According to Gooday (1993), *E. exigua* in the NW Atlantic is an opportunistic species feeding on phytodetritus. Its small size and thin-walled test is indicative of rapid reproduction when food supply to the sea-floor increases. In addition, *E. exigua* from the NW Atlantic is often associated with *A. glomerata*, which is also associated with our *Epistominella* spp. FA. However, unlike *E. exigua*, *A. glomerata* is not confined strictly to areas with significant influx of phytodetritus.

The *Epistominella* spp. FA. from the central trough of PIB bears resemblance to the *Epistominella* through assemblage found off the Larsen-A Ice Shelf (Ishman and Szymcek, 2003). Because of the presumed opportunistic character of important components of that assemblage, it was interpreted as adapted to a food-limited environment with seasonal food input. This interpretation may apply also to the *Epistominella* spp. FA. of PIB, where extended sea-ice cover allows only limited and strongly seasonal delivery of phytodetritus.

4.5.7. *Portatrochammina* spp. FA

This FA is defined by high scores of the complex taxon *Portatrochammina* spp., composed of *P. bipolaris*, *P. antarctica*, and *P. bullata* that are difficult to distinguish at immature stages. These three species appear to be distributed more or less throughout the study area. The only exceptions are *P. antarctica*, which completely dominates the *Portatrochammina* spp. assemablage in the Weddell Sea area, and the lack of *P. bullata* observed in Maxwell Bay and Admiralty Bay. The *Portatrochammina* spp. FA shows elevated PC scores of *A. glomerata* (Table 2) and also a significant positive correlation coefficient with *Reophax* cf. *R. spiculifer*, *Cystammina argentea*, and *Hormosinella* sp. (Table 4).

This FA is dominant in the NW Weddell Sea and at a few sites in PIB (Fig. 1), showing in both areas dominance of similar taxa and low percentages of calcareous species (Fig. 5). These similarities might suggest a single major factor affecting all sites dominated by

570 this FA. The *H* indices; however, differ significantly showing markedly lower diversities at
571 the three Weddell Sea sites relative to PIB sites (Fig. 4). Communities from the Weddell Sea
572 have rather low *H* values, while those of PIB are among the most diverse assemblages
573 studied. This difference suggests a presence of another factor that sets apart the
574 *Portatrochammina* spp. FA from the two areas.

575 While the fauna from PIB is well preserved, specimens from the northwestern
576 Weddell Sea show abundant signs of dissolution of calcareous foraminifera as well as poor
577 preservation of the dominant arenaceous forms, suggesting it is a relict assemblage. The poor
578 preservation of calcareous specimens is consistent with observations of Ishman and Szymcek
579 (2003) of assemblages dominated by *Portatrochammina* spp. from offshore of Larsen-A Ice
580 Shelf, which they interpreted as being modified by dissolution in areas lacking surface-water
581 carbonate production expressed by lack of planktonic foraminifera. Since our northwestern
582 Weddell Sea sites are located quite close to Larsen-A Ice Shelf, a similar interpretation seems
583 to apply to our data. The relatively low diversity of these samples, as compared with PIB,
584 could result from elimination of its calcareous species due to dissolution and disintegration of
585 more fragile agglutinated species shortly after burial.

586 The *Portatrochammina* spp. FA from the northwestern Weddell Sea, which is an area
587 influenced by Weddell Sea Water (Tokarczyk, 1987), resembles Violanti's (1996)
588 Assemblage III from deep-water settings of the Ross Sea and the Shallow Water Arenaceous
589 Facies of Anderson (1975a) from the southwestern Weddell Sea, which is dominated by
590 *Portatrochammina* with a significant percentages of *M. arenacea* and *A. glomerata*. In the
591 southwestern Weddell Sea, this assemblage is associated with a shallow CCD that results
592 from freezing and Saline Shelf Water formation, a situation that is consistent with the
593 northwestern Weddell Sea oceanographic setting.

594 The foraminiferal communities dominated by the *Portatrochammina* spp. FA in PIB
595 differ from those of the Weddell Sea in that they show significantly higher *H* values and they

include well-preserved agglutinated specimens, including fragile taxa. In the PIB area, there is a gradational transition between the *Epistominella* spp. FA, dominated by calcareous forms and associated with slightly coarser glacimarine sediments (Appendix 2) and the deeper water *Portatrochammina* spp. FA, which has a low occurrence of planktonic forams (Fig. 3) and occurs in very fine sediments that are nearly 100% finer than 63-μm fraction. It is apparent that this faunal change results from a different position with respect to the CCD, which is controlled by a less persistent CDW presence at shallower water depths dominated by the *Epistominella* spp. FA. The *Portatrochammina* spp. FA in PIB does not appear to be a relict assemblage, as we believe to be the case in the NW Weddell Sea.

4.5.8. *Miliammina arenacea* FA

The *Miliammina arenacea* FA shows high PC scores of *Spiroplectammina biformis* and *Paratrochammina bartrami* (Table 2), as well as significant correlation coefficient with the same species (Table 4). This FA is dominant at a few sites in Gerlache Strait and prominent at KC 10 in Hope Bay, where it is a minor assemblage component relative to the *Portatrochammina* spp. FA (Fig. 1). At sites dominated by *M. arenacea* FA, low percentages on calcareous foraminifera, no planktonics, and intermediate *H* values were noted (Figs. 3-5).

The principal species of this FA, *M. arenacea,* exhibits a uniquely high preservation potential (Schmiedl et al., 1997), which may strongly influence its domination in fossil assemblages (e.g., Majewski and Anderson, 2009). Other components of this FA, are *S. biformis* and *P. bartrami*, the former showing only slightly lower PC scores than the dominant species (Table 2). At all three sites (KC 31, KC 55, and KC 65) dominated by this assemblage (Fig. 1), the faunas are sparse and include incomplete specimens. Moreover, *P. bartrami* appears more robust than average agglutinated forms because of its thick organic lining supporting compact agglutinated outer test layers. These features indicate that this FA is at

621 least in part a residual assemblage, similar to the *Portatrochammina* spp. FA from the NW
622 Weddell Sea.
623 The *Miliammina arenacea* FA, dominates Gerlache Strait (Fig. 1), which is
624 characterized by organic-rich, diatomaceous sediments. It is also the dominant species in
625 areas where cold Saline Shelf Water occurs (Anderson, 1975a; Milam and Anderson, 1981;
626 Murray, 1991; Ishman and Domack, 1994) and is known to tolerate broad salinity fluctuations
627 (Ishman and Sperling 2002). It is also associated with diatom-rich sediments with elevated
628 organic content off Wilkes Land (Milam and Anderson, 1981) and off of Laren A Ice Shelf
629 (Ishman and Szymcek 2003). Similar association with organic-rich, low-oxygen conditions
630 were interpreted for *S. biformis* in Norwegian fjords (Sen Gupta and Machain-Castillo, 1993).
631 The sheltered location of the Gerlache Strait is conducive to a stable uppermost water layer,
632 which in turn supports strong primary production and delivery of plentiful organic matter to
633 the sea floor. The dominant presence of calcareous foraminifera at several sites located at
634 similar water depths and locations not distant from sites dominated by the *M. arenacea* FA
635 indicates that local factors influence this FA.
636
637 **4.6. The main factors influencing foraminiferal assemblages from coastal West**
638 **Antarctica**
639 Near-shore, relatively shallow (a few hundred meter of water-depth) settings are
640 characterized by a considerable range of calcareous foraminifera. The diversity of sub-fossil
641 assemblages generally increases offshore and with increasing water-depth (Fig. 4), reflecting
642 decreasing turbidity and less punctuated food supply. This trend is disrupted by poor
643 preservation of calcareous species. Of principal importance is variable preservation of
644 calcareous tests affected by corrosive water masses and/or acidic pore waters. Thus,
645 foraminiferal assemblages composed exclusively of agglutinated forms should be treated with
646 caution, as they are potentially impoverished by taphonomic processes.

The exact cause of dissolution and depth of the dissolution boundary varies spatially in response to different oceanographic conditions and differences in pore water acidity. The *Portatrochammina* spp. FA provides a good example (see distribution of triangles indicating this FA on Fig. 4). In the PIB area, it is a highly diverse, well preserved assemblage devoid of calcareous forms because of prolonged exposure to corrosive CDW. In the Weddell Sea, this FA is poorly preserved and reduced in diversity, again depleted in calcareous species, but in this case associated with corrosive Saline Shelf Water along with possible acidic pore water.

The *M. arenacea* FA, which is dominated by this relatively robust agglutinated species, is regarded as a residual assemblage. It corresponds to conditions of exceptionally high primary productivity in sheltered locations with a stable upper water column. However, assemblages strongly dominated by agglutinated forms are not always impoverished, as exemplified by *Portatrochammina* spp. in PIB. In relatively deep water settings with well-ventilated bottom waters and low primary production, assemblages with very minor calcareous elements are common.

Off coastal West Antarctica, the most important factor influencing benthic foraminiferal assemblages is the strong seasonality of primary production. Its impact is exhibited by the common presence of opportunistic, detritus feeding foraminifera, including the index taxa of the *F. fusiformis*, *Epistominella* spp., and presumably also *B. pseudopunctata* FAs (Fig. 1). These assemblages are composed of species that are minute in size and have thin transparent walls. These features reflect their opportunistic nature and ability for rapid growth and reproduction (Gooday, 1993). Such behavior gives them a clear advantage in habitats with seasonal food supply, which is typical for Antarctic coastal seas. The same group of opportunistic minute benthic foraminifera, which are not used for defining FAs, is also important within the remaining FAs (Appendix 1). In some cases the *B. pseudopunctata* and *F. fusiformis* FAs may cluster together. They seem to differ only by the former being more tolerant to coastal glaciers that increases turbidity and terrigenous input as

673 well as a less stable upper water column that slightly limits productivity. The *Epistominella*
674 spp. FA in PIB, on the other hand, is typical for more open-water areas with strongly seasonal
675 and reduced productivity, caused by prolonged sea-ice duration, accompanied by occasional
676 CDW influence as an additional factor.

677 The *G. biora*, *A. echolsi*, and *B. aculeata* FAs are dominated by calcareous
678 foraminifera and by species with more massive test walls, suggesting a less opportunistic life
679 style and more stable conditions, at least in terms of food supply. The *G. biora* FAs is found
680 only in areas significantly impacted by glacier sedimentation. These are areas of increased
681 water turbidity that impacts primary production by limiting the depth of the photic zone on
682 one side and nutrient delivery on the other. The *A. echolsi* and *B. aculeata* FAs are present in
683 progressively more open-water habitats with less punctuated food supply and less turbid
684 waters.

685 The distribution of *B. aculeata* individuals is of special importance. It correlates well
686 with the boundary interpreted by Ishman and Domack (1994) and Shevenell and Kennett
687 (2002) southeast of Anvers Island between deep water-masses influenced by Weddell Sea
688 Transitional Water to NE and Upper Circumpolar Deep Water to SW (Fig 6). Thus, our study
689 confirms that *B. aculeata* favors conditions associated with CDW presence. However, it is
690 also important to note that our CTD data (Fig. 2) and the lack of *B. aculeata* in Maxwell and
691 Admiralty bays, including a lack at site KC 1A from 488 mwd (Fig. 6), does not support
692 CDW influence on the Bransfield Strait side of the South Shetland Islands, as interpreted by
693 Shevenell and Kennett (2002). Our data are consistent with the presence of Weddell Sea
694 Transitional Water as interpreted by Ishman and Domack (1994).

695 Finally, the *Epistominella* spp. and *Portatrochammina* spp. FAs occur in areas where
696 warm CDW flows onto the continental shelf, as well, specifically in PIB (Fig. 1). These same
697 FAs are associated with strongly seasonal and limited productivity within this area. The

Portatrochammina spp. occurs also in the northwestern Weddell Sea (Fig. 1), which is under influence of Weddell Sea Water and not CDW.

5. Conclusions

The eight FAs recognized in this work reflect large variability in benthic foraminiferal assemblages and associated environmental conditions. Six FAs are dominated by calcareous taxa and may be arranged more or less according to decreasing glacial influence. The last two FAs, dominated by arenaceous taxa, indicate corrosive conditions.

The most important factor impacting benthic foraminiferal assemblages in West Antarctic coastal settings is the variable food supply and its seasonal delivery. Significant terrigenous sedimentation may be important as well but it is also linked to the food factor as turbid water affects primary production. Temperatures and salinities of Antarctic coastal waters are not as variable as at lower latitudes, but the presence of warm deep-water water masses that are corrosive to carbonate, is also important. Three of the faunal assemblages identified in this study: *Bulimina aculeata, Epistominella* spp., and *Portatrochammina* spp, FAs, occur in areas were Circumpolar Deep Water is known to impinge onto the continental shelf. Thus, these assemblages may provide a paleoceanographic tool for studying this important process.

Our results confirm that some fossil assemblages may be poorly representative of "living" assemblages due to poor preservation in some settings. Assemblages dominated by agglutinated foraminifera reflect conditions corrosive to carbonate but may or may not be residual, i.e., depleted in number of species.

Acknowledgements

JSW and JBA were funded by the National Science Foundation Office of Polar Programs grant 0837925. We thank the captains, crews, and scientific parties of *R/V Nathaniel B.*

724 *Palmer* (cruises NBP0502, NBP0602A, and NBP0703) and *R/V Oden* (OSO 0910) and the
725 Antarctic Marine Research Facility at Florida State University for their assistance. We thank
726 Alex Orsi for providing CTD data from Ferrero Bay. We would like to thank two anonymous
727 reviewers for their comments.
728
729 **References**
730 Allen, C.S., Oakes-Fretwell, L., Anderson, J.B., Hodgson, D.A., 2010. A record of Holocene
731 glacial and oceanographic variability in Neny Fjord, Antarctic Peninsula. Holocene,
732 20, 551–564.
733 Alve, E., 1994. Opportunistic features of the foraminifer Stainforthia fusiformis (Williamson):
734 evidence from Frierfjord, Norway. Journal of Micropalaeontology 13, 24.
735 Anderson, J.B., 1975a. Ecology and distribution of foraminifera in the Weddell Sea of
736 Antarctica. Micropaleontology 21, 69–96.
737 Anderson, J.B., 1975b. Factors controlling $CaCO_3$ dissolution in the Weddell Sea from
738 foraminiferal distribution patterns. Marine Geology 19, 315–332.
739 Barnard, A., Wellner, J.S., Anderson, J.B., 2014. Small but significant late Holocene regional
740 climate change documented in high-resolution sediment core from the Bransfield
741 Strait, Antarctic Peninsula. Polar Research 33, 17236.
742 Bárcena, M.A., Fabrés, J., Isla, E., Flores, J.A., Sierro, F.J., Canals, M., Palanques, A., 2006.
743 Holocene neoglacial events in the Bransfield Strait (Antarctica). Palaeoceanographic
744 and palaeoclimatic significance. Scientia Marina 70, 607–619.
745 Boldt, K., Nittrouer, C., Hallet, B., Koppes, M., Forrest, B., Wellner, J., Anderson, J., 2013.
746 Modern rates of glacial sediment accumulation along a 15° S-N transect: in fjords of
747 the Antarctic Peninsula and southern Chile. Journal of Geophysical Research-Earth
748 Surface 118, 1–17.

749 Cape, M., Vernet, M., Kahru, M., Preen, G., 2014. Polynya dynamics drive primary
750 production in the Larsen A and B embayments following ice shelf collapse, Journal of
751 Geophysical Research-Oceans 119, 572–594.
752 Chang, S.-K., Yoon, H.I., 1995. Foraminiferal assemblages from bottom sediments at Marian
753 Cove, South Shetland Islands, West Antarctica. Marine Micropaleontology 26, 223–
754 232.
755 Comiso, J., 2000. Variability and trends in Antarctic surface temperatures from in situ and
756 satellite infrared measurements. Journal of Climate 13, 1674–1696.
757 Domack, E.W., Ishman, S., 1993. Oceanographic and physiographic controls on modern
758 sedimentation within Antarctic fjords. Geological Society of America Bulletin 105,
759 1175–1189.
760 Ducklow, H.W., Baker, K., Martinson, D.G., Quetin, L.B., Ross, R.M., Smith, R.C.,
761 Stammerjohn, S.E., Vernet, M., Fraser, W., 2007. Marine pelagic ecosystems: the
762 West Antarctic Penisnula, Philosphical Transactions of the Royal Society: Biological
763 Sciences 362, 67–94.
764 Earland, A., 1934. Foraminifera. Part III. The Falklands sector of the Antarctic (excluding
765 South Georgia). Discovery Reports 10, 1–208.
766 Finger, K.L., Lipps, J.H., 1981. Foraminiferal decimation and repopulation in an active
767 volcanic caldera, Deception Island, Antarctica. Micropaleonthology 27, 111–139.
768 Garibotti, I.A., Vernet, M., Ferrario, M.E., Smith, R.C., Ross, R.M., Quetin, L.B., 2003.
769 Phytoplankton spatial distribution patterns along the western Antarctic Peninsula
770 (Southern Ocean). Marine Ecology Progress Series 261, 21–39
771 Gooday, A.J., 1993. Deep-sea benthic foraminiferal species which exploit phytodetritus:
772 characteristic features and controls on distribution. Marine Micropaleontology 22,
773 187–205.

774 Gooday, A.J., Rothe, N., Bowser, S.S., Pawlowski J. 2014. Benthic Foraminifera. In: De
775 Broyer, C., Koubbi, P., Griffiths, H.J., et al. (eds.). Biogeographic Atlas of the Southern
776 Ocean. Scientific Committee on Antarctic Research, Cambridge, pp 74–82
777 Gordon, A.L., Chen, C.T.A., Metcalf, W.G., 1984. Winter mixed layer entrainment of
778 Weddell Deep Water. Journal of Geophysical Research: Oceans 89(C1), 637–640.
779 Gray, S.C., Sturz, A., Bruns, M.D., Marzan, R.L., Dougherty, D., Law, H.B., Brackett, J.E.,
780 Marcou, M., 2003. Composition and distribution of sediments and benthic foraminifera
781 in a submerged caldera after 30 years of volcanic quiescence. Deep-Sea Research II 50,
782 1727–1751.
783 Griffith, T.W., Anderson, J.B., 1989. Climatic control of sedimentation in bays and fjords of
784 the northern Antarctic Peninsula. Marine Geology 85, 181–204.
785 Hofmann, E.E., Klinck, J.M., 1998. Hydrography and circulation of the Antarctic continental
786 shelf: 150E to the Greenwich meridian. In: Robinson A. R., and Kenneth H. Brink
787 (Ed.) The Sea, vol 11. John Wiley & Sons, Inc., 997–1042.
788 Hofmann, E.E., Klinck, J.M., Lascara, C.M., Smith, D.A., 1996. Water mass distribution and
789 circulation west of the Antarctic Peninsula and including Bransfield Strait. In: Ross
790 R.M., Hofmann E.E. and Quetin L.B. (eds), Foundations for Ecological Research
791 West of the Antarctic Peninsula. Antarctic Research Serries 70, 81–104.
792 Hughes, T., 1981. The weak underbelly of the West Antarctic Ice Sheet. Journal of
793 Glaciology 27, 518–525.
794 Ishman, S.E., Domack, E.W., 1994. Oceanographic controls on benthic foraminifers from the
795 Bellingshausen margin of the Antarctic Peninsula. Marine Micropaleontology 24,
796 119–155.
797 Ishman, S.E., Sperling, M.R., 2002. Benthic foraminiferal record of Holocene deep-water
798 evolution in the Palmer Deep, western Antarctic Peninsula. Geology 30, 435–438.

799 Ishman, S.E., Szymcek, P., 2003. Foraminiferal distributions in the former Larsen-A Ice Shelf
800 and Prince Gustav Channel region, eastern Antarctic Peninsula margin: A baseline for
801 Holocene paleoenvironmental interpretation. Antarctic Research Series 79, 239–260.
802 Jacobs, S.S., Jenkins, A., Giulivi, C.F., Dutrieux, P., 2011. Stronger ocean circulation and
803 increased melting under Pine Island Glacier ice shelf. Nature Geoscience 4, 519–523.
804 Jacobs, S., Jenkins, A., Hellmer, H., Giulivi, C., Nitsche, F., Huber, B., Guerrero, R., 2012.
805 The Amundsen Sea and the Antarctic Ice Sheet. Oceanography 25, 154–163.
806 Kang, S.-H., Fryxell, G.A., 1993. Phytoplankton in the Weddell Sea, Antarctica.
807 Composition, abundance and distribution in the water-column assemblages of the
808 marginal ice-edge zone during austral summer. Marine Biology 116, 335–348.
809 Kang, S.-H., Kim, D.Y., Kang, J.S., Lee, M.Y., Lee, S.H., 1995 Antarctic phytoplankton in
810 the eastern Bransfield region and in the northwestern Weddell Sea marginal ice zone
811 during austral summer. Korean Journal of Polar Research 6, 1–30.
812 Kang, S.-H., Kang, J.S., Lee, S., Chung, K.H., Kim, D., Park, M.G., 2001 Antarctic
813 phytoplankton assemblages in the marginal ice zone of the northwestern Weddell Sea.
814 Journal of Plankton Research 23, 333–352.
815 Kellogg, D.E., Kellogg, T.B., 1987. Microfossil distribution in modern Amundsen Sea
816 sediments. Marine Micropaleontology 12, 203–222.
817 King, J.C., Turner, J., Marshall, G.J., Connolley, W.M., Lachlan-Cope, T.A., 2003. Antarctic
818 Peninsula climate variability and its causes as revealed by instrumental records.
819 Antarctic Research Series 79, 17–30.
820 Kruszewski, G., 2002. Zlodzenie Zatoki Admiralicji – przebieg i uwarunkowania.
821 Wydawnictwo Uczelniane Akademii Morskiej, Gdynia. 123 pp. (in Polish)
822 Lipski, M., 1987. Variations of physical conditions, nutrient and chlorophyll a contents in
823 Admiralty Bay (King George Island, South Shetland Islands, 1979). Polish Polar
824 Research 8, 307–332.

825 Loeblich, A.R., Tappan, H., 1987. Foraminiferal Genera and their Classification. Van
826 Nostrand Reinhold Company, New York: 970 pp.
827 Mackensen, A., Grobe, H., Kuhn, G., Fütterer, D.K., 1990. Benthic foraminiferal assemblages
828 from the eastern Weddell Sea between 68 and 73°S: Distribution, ecology and
829 fossilization potential. Marine Micropaleontology 16, 241–283.
830 Majewski, W., 2005. Benthic foraminiferal communities: distribution and ecology in
831 Admiralty Bay, King George Island, West Antarctica. Polish Polar Research 26, 159–
832 214.
833 Majewski, W., 2010. Benthic foraminifera from West Antarctic fiord environments: An
834 overview. Polish Polar Research 31, 61–82.
835 Majewski, W., 2013. Benthic foraminifera from Pine Island and Ferrero bays, Amundsen Sea.
836 Polish Polar Research 34 (2): 169–200.
837 Majewski, W., Anderson, J.B., 2009. Holocene foraminiferal assemblages from Firth of Tay,
838 Antarctic Peninsula: Paleoclimate implications. Marine Micropaleontology 73, 135–
839 247.
840 Majewski, W., Pawlowski, J., 2010. Morphologic and molecular diversity of the foraminiferal
841 genus Globocassidulina in Admiralty Bay, West Antarctica. Antarctic Science 22,
842 271–281.
843 Majewski, W., Tatur, A., 2009. A new Antarctic foraminiferal species for detecting climate
844 change in sub-Recent glacier-proximal sediments. Antarctic Science 5, 439–448.
845 Majewski, W., Lecroq, B., Sinniger, F., Pawłowski, J., 2007. Monothalamous foraminifera
846 from Admiralty Bay, King George Island, West Antarctica. Polish Polar Research 28,
847 187–210.
848 Majewski, W., Wellner, J.S., Szczuciński, W., Anderson, J.B., 2012. Holocene oceanographic
849 and glacial changes recorded in Maxwell Bay, West Antarctica. Marine Geology 326–
850 328, 67–79.

851 Malmgren, B.A., Haq, B.U., 1982, Assessment of quantitative techniques in
852 paleobiogeography. Marine Micropaleontology 7, 213–236.
853 Martinson, D.G., Stammerjohn, S.E., Iannuzzi, R.A., Smith, R.C., Vernet, M., 2008. Western
854 Antarctic Peninsula physical oceanography and spatio-temporal variability. Deep Sea
855 Research Part II: Topical Studies in Oceanography 55, 1964–1987.
856 Mayer, M., 2000. Zur Ökologie der Benthos−Foraminiferen der Potter Cove (King George
857 Island, Antarktis). Berichte zur Polarforschung 353, 1–126.
858 Meredith, M.P., King, J.C., 2005. Climate change in the ocean to the west of the Antarctic
859 Peninsula during the second half of the 20th century. Geophysical Research Letters 32,
860 L19604.
861 Michalchuk, B., Anderson, J.B., Wellner, J.S., Manley, P.L., Bohaty, S., Majewski, W., 2009.
862 Holocene climate and glacial history of the northeastern Antarctic Peninsula: the
863 marine sedimentary record from a long SHALDRIL core. Quaternary Science
864 Reviews 28, 3049–3065.
865 Milam, R.W., Anderson, J.B., 1981. Distribution and ecology of recent benthonic
866 foraminifera of the Adelie-George V continental shelf and slope, Antarctica. Marine
867 Micropaleontology 6, 297–325.
868 Milliken, K.T., Anderson, J.B., Wellner, J.S., Bohaty, S., Manley, P. 2009 High-resolution
869 Holocene climate record from Maxwell Bay, South Shetland Islands, Antarctica.
870 Geological Society of America Bulletin 121, 1711–1725.
871 Minzoni, R., Anderson, J.B., Fernandez, R., Wellner J.S., in press, Holocene climate, ocean,
872 and cryosphere interactions in the eastern Antarctic Peninsula: High-resolution, multi-
873 proxy investigation of Herbert-Croft Fjord, James Ross Island, Quaternary Science
874 Reviews.

875 Murray, J.W., Pudsey, C.J., 2004. Living (stained) and dead foraminifera from the newly ice-
876 free Larsen Ice Shelf, Weddell See, Antarctica: ecology and taphonomy. Marine
877 Micropaleontology 53, 67–81.
878 Murray, J.W., 1991. Ecology and palaeoecology of benthic foraminifera. Longman Scientific
879 and Technical. 397 pp.
880 Orsi, A.H., Whitworth, III T., Nowlin, Jr. W.D., 1995. On the meridional extent and fronts of
881 the Antarctic circumpolar current. Deep Sea Research 42(5), 641–673.
882 Parkinson, C.L., Cavalieri, D.J., 2012. Antarctic sea ice variability and trends, 1979–2010.
883 The Cryosphere 6, 871–880.
884 Pflum, C.E., 1966. The distribution of the foraminifera of the eastern Ross Sea, Amundsen
885 Sea and Bellingshausen Sea, Antarctica. Bulletins of American Paleontology 50 (226),
886 151–209.
887 Reynolds, J.M., 1981. The distribution of mean annual temperatures in the Antarctic
888 Peninsula. British Antarctic Survey Bulletin 54, 122–33.
889 Rodrigues, A.R., Maluf, J.C.C., Braga, E.D.S., Eichler, B.B., 2010. Recent benthic
890 foraminiferal distribution and related environmental factors in Ezcurra Inlet, King
891 George Island, Antarctica. Antarctic Science 22, 343–360.
892 Schmiedl, G., Mackensen, A., Müller, P.J., 1997. Recent benthic foraminifera from the
893 eastern South Atlantic Ocean: Dependence on food supply and water masses. Marine
894 Micropaleontology 32, 249–287.
895 Sen Gupta, B.K., Machain-Castillo, M.L., 1993. Benthic foraminifera in oxygen-poor
896 habitats. Marine Micropaleontology 20, 183–201.
897 Shevenell, A.W., Kennett, J.P., 2002. Antarctic Holocene climate change: A benthic
898 foraminiferal stable isotope record from Palmer Deep. Paleoceanography 17, 1–13.
899 Świło, M., Majewski, W., Anderson, J.B., Minzoni, R., In prep. Diatom assemblages from
900 coastal settings of West Antarctica.

Szafrański, Z., Lipski, M., 1982. Characteristics of water temperature and salinity at Admiralty Bay (King George Island, South Shetland Islands, Antarctic) during the austral summer 1978/1979. Polish Polar Research 3, 7–24.

Tokaczyk, R., 1987. Classification of water masses in the Bransfield Strait and southern part of the Drake Passage using a method of statistical multidimensional analysis. Polish Polar Research 8, 333–366.

Turner, J., Colwell, S.R., Marshall, G.J., Lachlan-Cope, T.A., Carelton, A.M., Jones, P.D., Lagun, V., Reid, P.A., Iagovkina, S., 2005. Antarctic climate change during the last 50 years. International Journal of Climatology 25, 279–294.

Vaughan, D.G., Marshall, G.J., Connolley, W.M., King, J.C., Mulvaney, R., 2001. Climate Change: Devil in the Detail. Science 293, 1777–1779.

Vaughan, D.G., Marshall, G.J., Connolley, W.M., Parkinson, C.L., Mulvaney, R., Hodgson, D.A., King, J.C., Pudsey, C.J., Turner, J., 2003, Recent rapid regional climate warming on the Antarctic Peninsula. Climatic Change 60, 243–274.

Venegas, S.A., Drinkwater, M.R., 2001. Sea ice, atmosphere and upper ocean variability in the Weddell Sea, Antarctica. Journal of Geophysical Research 106 (C8), 16747–16766.

Violanti, D., 1996. Taxonomy and distribution of recent benthic foraminifers from Terra Nova Bay (Ross Sea, Antarctica), Oceanographic Campaign 1987/1988. Palaeontographia Italica 83, 25–71.

Table 1. Sampling sites.

Table 2. Foraminiferal PC scores. Taxa important for particular FAs are in bold.

Table 3. Foraminiferal PC loadings. FA values important for particular sites are in bold.

Table 4. Pearson's correlation coefficients between various foraminiferal indices. Significant correlation coefficients highlighted in bold.

927 Fig. 1. Map of the Antarctic Peninsula showing the location of sediment samples and the
928 distribution distribution of foraminiferal assemblages (FAs). Schematic oceanic circulation
929 after Shevenell and Kennett (2002). Abbreviated location names: AdB – Admiralty Bay, AnB
930 – Andvord Bay, BB – Beascochea Bay, BC – Brialmont Cove, FlB – Flandres Bay, FB –
931 Ferrero Bay, GS – Gerlache Strait, LB – Laperère Bay, MB – Maxwell Bay.
932 Fig. 2. CTD data collected during NBP0703 and Oden cruises highlighting the basic water
933 mass structure in each area of this study.
934 Fig. 3. Foraminiferal p/b ratios. Outlined assemblages are from the same regions. Note
935 explanation of foraminiferal assemblage (FA) symbols.
936 Fig. 4. Foraminiferal Shannon diversity index plotted against bathymetry of sampling sites.
937 Outlined assemblages are from the same regions. For explanation of FA symbols, see Fig. 1
938 or Fig. 3.
939 Fig. 5. Percent calcareous benthic foraminifera. Outlined assemblages are from the same
940 regions. For explanation of FA symbols, see Fig. 1 or Fig. 3.
941 Fig. 6. Distribution of *Bulimina aculeata*, which according to Ishman and Domack (1994)
942 indicate presence of CDW. For complete schematic circulation after Shevenell and Kennett
943 (2002) see Fig. 1.
944
945 Appendix 1. Foraminiferal census data.
946 Appendix 2. Foraminiferal assemblages (FAs) with granulometric data.
947
948
949

Figure(s)

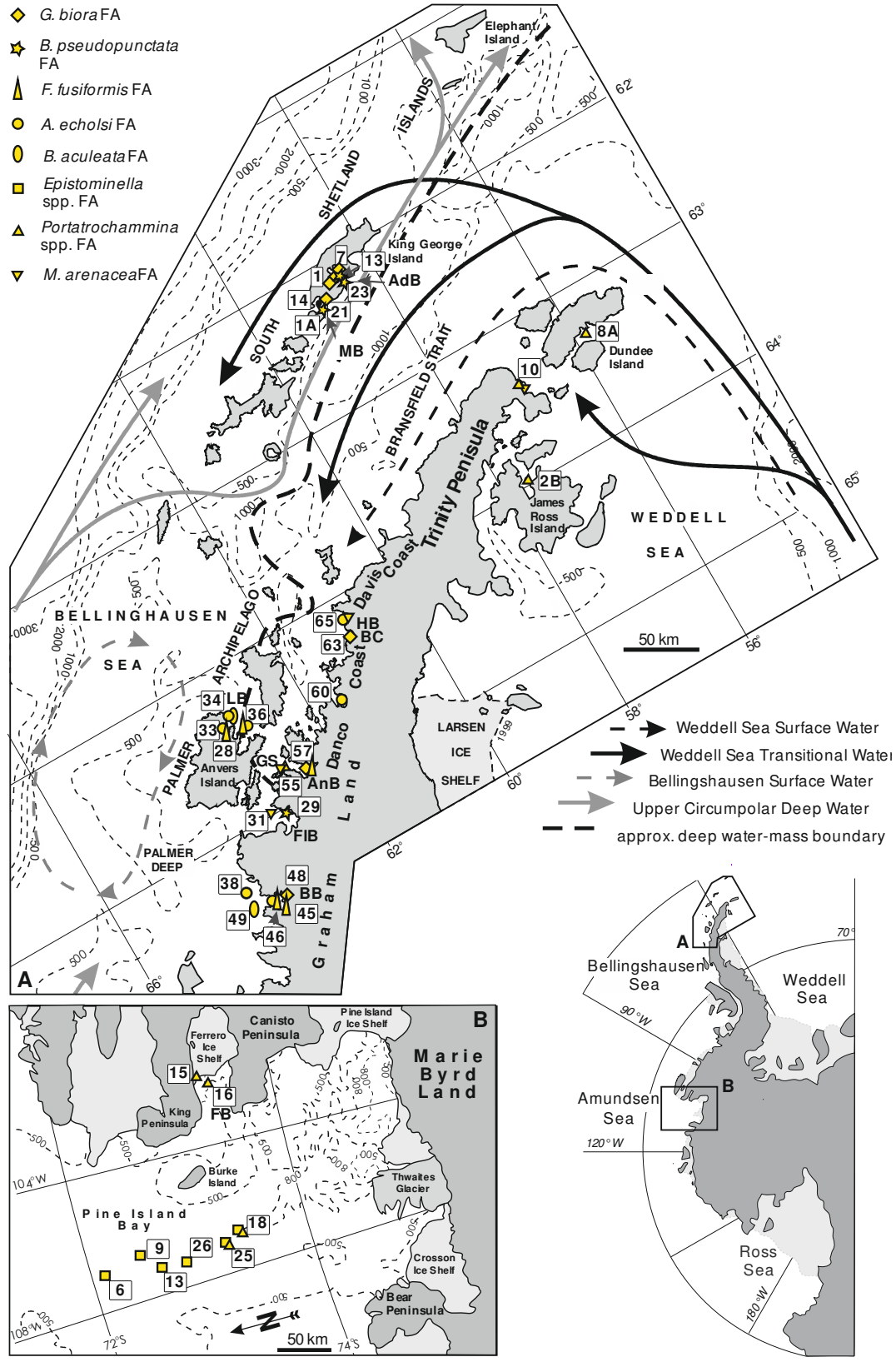

Fig. 1. Map of the Antarctic Peninsula showing the location of sediment samples and the distribution distribution of foraminiferal assemblages (FAs). Schematic oceanic circulation after Shevenell and Kennett (2002). Abbreviated location names: AdB – Admiralty Bay, AnB – Andvord Bay, BB – Beascochea Bay, BC – Brialmont Cove, FlB – Flandres Bay, FB – Ferrero Bay, GS – Gerlache Strait, LB – Laperère Bay, MB – Maxwell Bay.

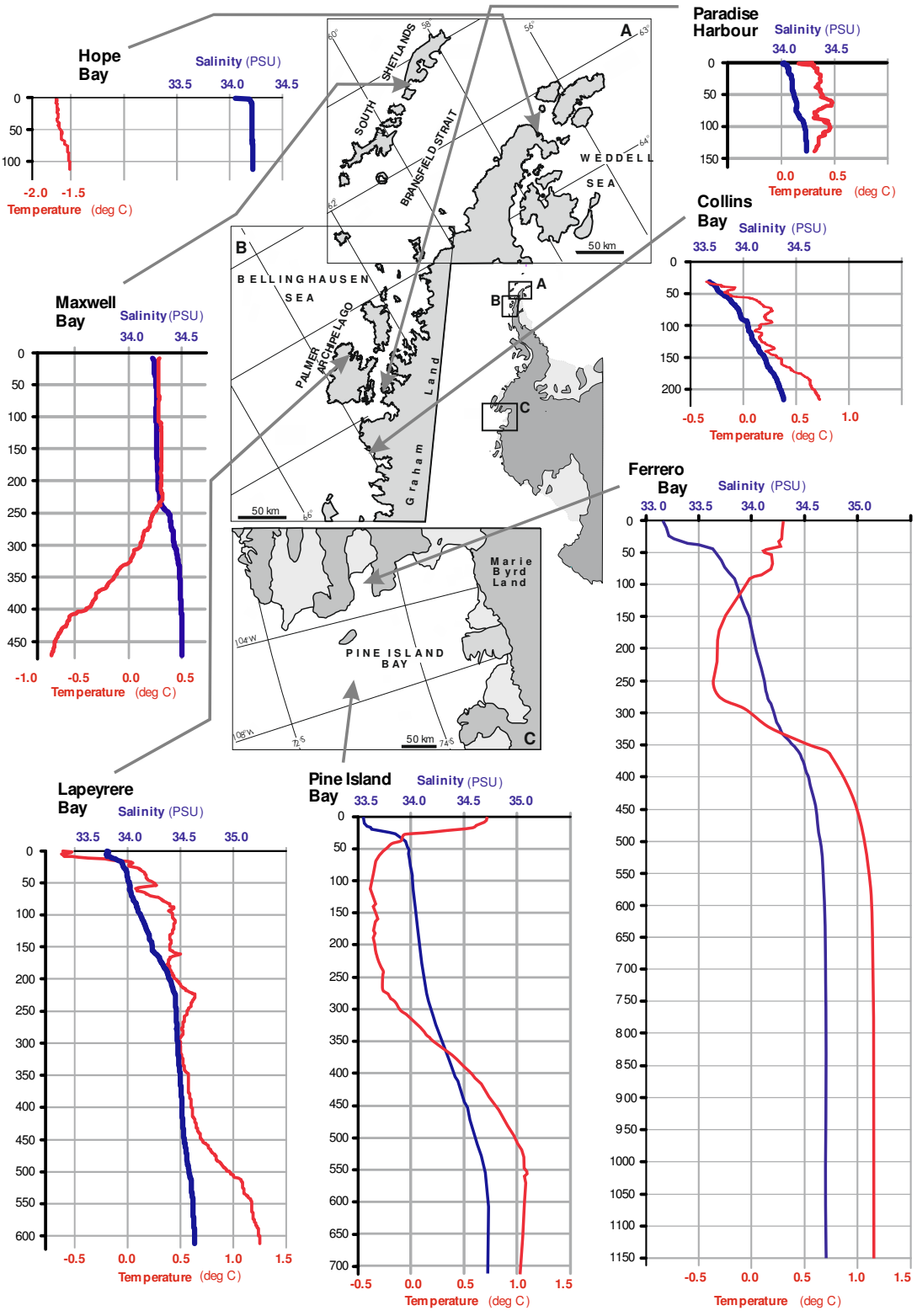

Fig. 2. CTD data collected during NBP0703 and Oden cruises highlighting the basic water mass structure in each area of this study.

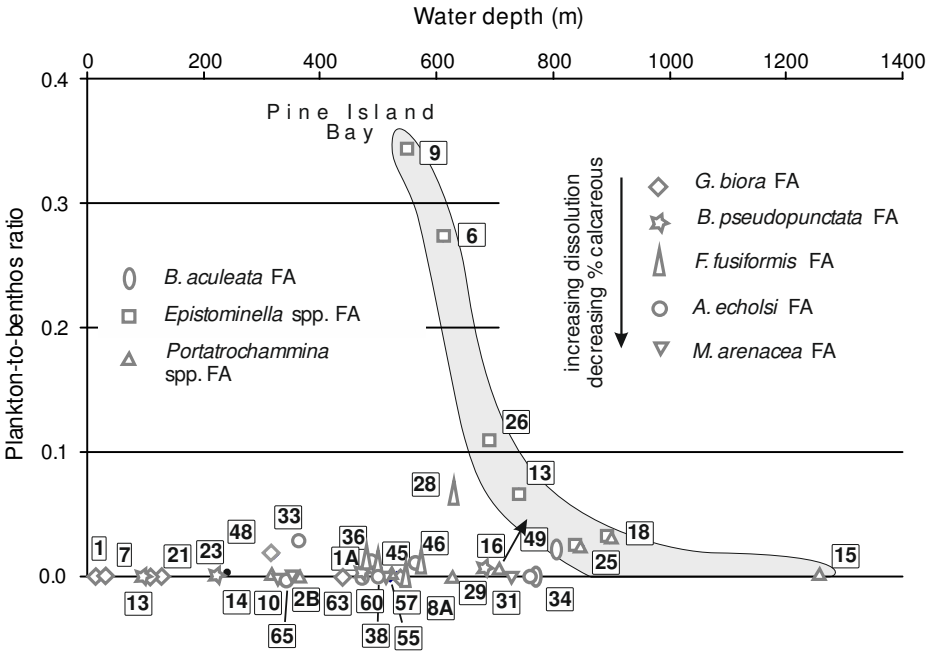

Fig. 3. Foraminiferal p/b ratios. Outlined assemblages are from the same regions. Note explanation of foraminiferal assemblage (FA) symbols.

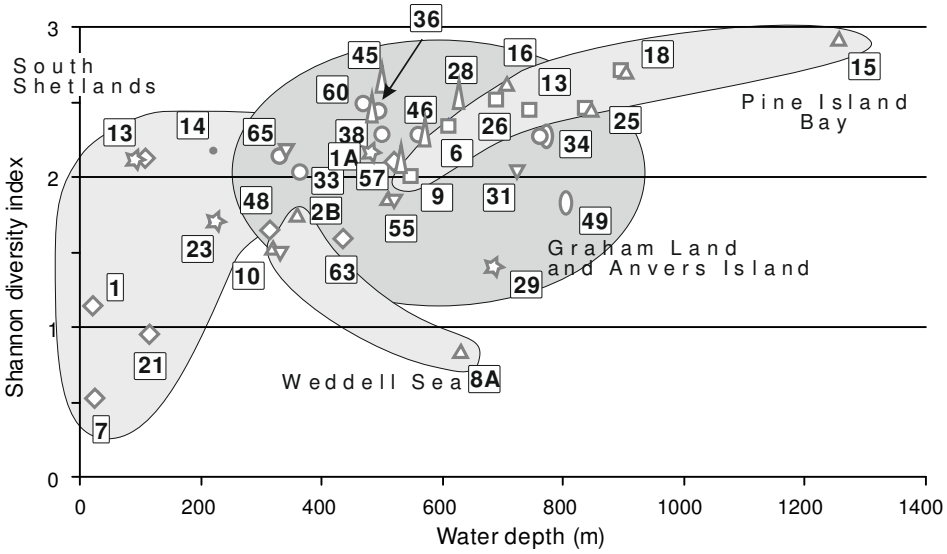

Fig. 4. Foraminiferal Shannon diversity index plotted against bathymetry of sampling sites. Outlined assemblages are from the same regions. For explanation of FA symbols, see Fig. 1 or Fig. 3.

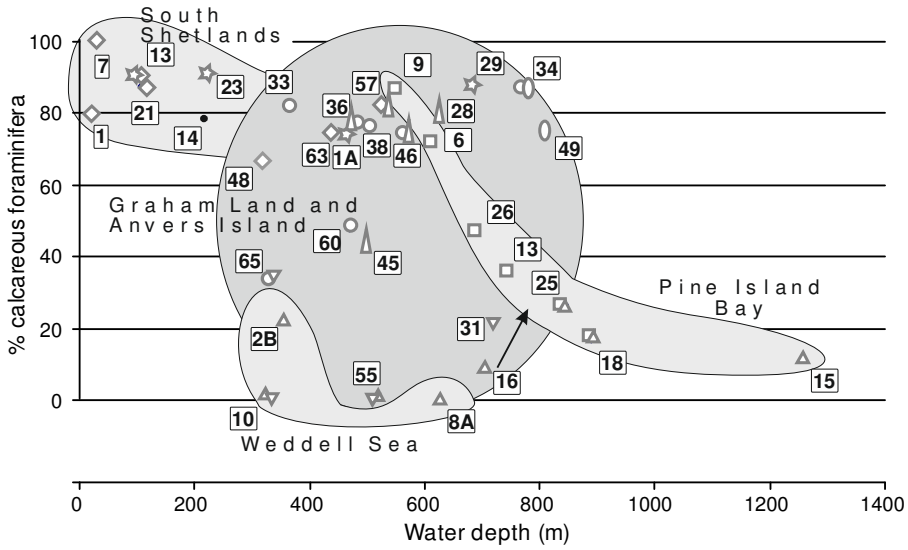

Fig. 5. Percent calcareous benthic foraminifera. Outlined assemblages are from the same regions. For explanation of FA symbols, see Fig. 1 or Fig. 3.

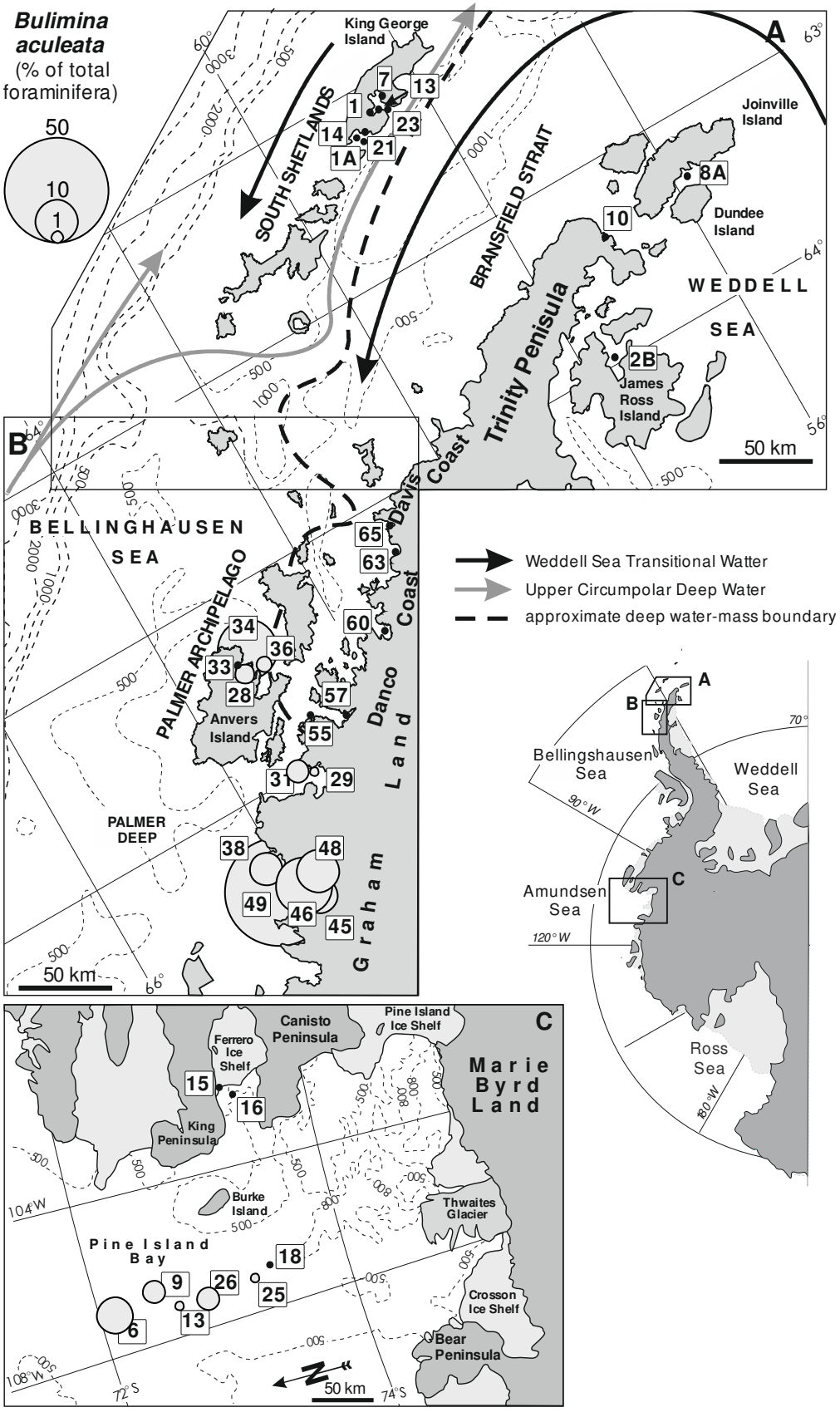

Fig. 6. Distribution of *Bulimina aculeata*, which according to Ishman and Domack (1994) indicate presence of CDW. For complete schematic circulation after Shevenell and Kennett (2002) see Fig. 1.

Table (S)

Table 1. Sampling sites.

Sample	Water depth (m)	Latitude	Longitude	Location
KG-1	20	62°11.00' S	58°37.31' W	Admiralty Bay
KG-7	30	62°06.22' S	58°19.68' W	Admiralty Bay
KG-13	108	62°09.46' S	58°29.74' W	Admiralty Bay
KG-23	223	62°13.36' S	58°22.89' W	Admiralty Bay
NBP0502-KC-1A	488	62° 16.93' S	58° 45.23' W	Maxwell Bay
NBP0502-KC-2B	359	63° 58.26' S	57° 45.51' W	Herbert Sound
NBP0602A-KC-8A	629	63° 20.57' S	55° 53.20' W	Firth of Tay
NBP0703-KC-10	323	63° 23.14' S	57° 00.58' W	Hope Bay
NBP0703-KC-14	220	63° 11.79' S	58° 50.81' W	Maxwell Bay, Colin Harbour
NBP0703-KC-21	112	62° 12.32' S	58° 44.31' W	Maxwell Bay, Marian Cove
NBP0703-KC-28	627	64° 24.10' S	63° 15.14' W	Anvers Island, Lapeyrère Bay
NBP0703-KC-29	684	65° 03.09' S	63° 06.19' W	Flandres Bay
NBP0703-KC-31	723	65° 00.17' S	63° 18.86' W	Flandres Bay
NPB0703-KC-33	363	64° 22.40' S	63° 17.32' W	Anvers Island, Lapeyrère Bay
NBP0703-KC-34	767	64° 20.11' S	63° 05.88' W	Anvers Island, Lapeyrère Bay
NBP0703-KC-36	486	64° 26.22' S	63° 00.82' W	Anvers Island, Lapeyrère Bay
NBP0703-KC-38	501	65° 20.64' S	64° 17.19' W	Collins Bay
NBP0703-KC-45	499	65° 35.32' S	63° 49.70' W	Beascochea Bay
NBP0703-KC-46	567	65° 31.79' S	63° 54.63' W	Beascochea Bay
NBP0703-KC-48	318	65° 30.57' S	63° 42.50' W	Beascochea Bay
NPB0703-KC-49	807	65° 28.79' S	64° 18.29' W	Beascochea Bay
NBP0703-KC-55	519	64° 46.86' S	62° 52.17' W	Andrord Bay
NBP0703-KC-57	532	64° 52.35' S	62° 25.50' W	Andrord Bay
NBP0703-KC-60	470	64° 37.93' S	62° 31.16' W	Charlote Bay
NBP0703-KC-63	438	64° 17.42' S	60° 58.91' W	Hughes Bay
NBP0703-KC-65	340	64° 09.43' S	60° 51.77' W	Hughes Bay
OSO0910-KC-6	612	72° 07.95' S	106° 54.60' W	central Pine Island Bay
OSO0910-KC-9	548	72° 29.20' S	106° 38.34' W	central Pine Island Bay
OSO0910-KC-13	742	72° 38.44' S	107° 10.12' W	central Pine Island Bay
OSO0910-KC-15	1257	73° 21.62' S	101° 50.17' W	Ferrero Bay
OSO0910-KC-16	706	73° 27.24' S	102° 04.75' W	Ferrero Bay
OSO0910-KC-18	894	73° 23.01' S	106° 52.26' W	central Pine Island Bay
OSO0910-KC-25	838	73° 15.42' S	107° 06.34' W	central Pine Island Bay
OSO0910-KC-26	689	72° 51.87' S	107° 13.34' W	central Pine Island Bay

Table 2. Foraminiferal PC scores. Taxa important for particular FAs are in bold.

	***Portatrochammina* spp. FA**	***Epistominella* spp. FA**	***G. biora* FA**	***A. echolsi* FA**	***B. pseudopunctata* FA**	***F. fusiformis* FA**	***M. arenacea* FA**	***B. aculeata FA***
Percent of total variance explained	15.87	13.94	13.74	11.55	10.64	8.60	6.86	4.47
Rhabdammina spp.	0.078	0.843	-0.187	0.597	-0.677	-0.638	-0.136	-0.969
Psammosphaera fusca	-0.188	-0.380	0.272	-0.361	-0.184	-0.374	-0.297	-0.129
Lagenammina arenulata	-0.507	-0.321	-0.313	-0.003	-0.009	-0.224	0.711	0.248
Reophax subdentaliniformis	-0.270	-0.255	0.407	0.085	-0.460	-0.312	0.472	0.361
Reophax scorpiurus	-0.394	-0.350	-0.298	-0.161	-0.223	-0.278	-0.239	0.007
Reophax cf. *R. spiculifer*	-0.204	-0.296	-0.299	-0.292	-0.210	-0.352	-0.291	-0.296
Nodulina cf. *N. dentaliniformis*	-0.361	-0.362	-0.266	-0.189	-0.178	-0.329	-0.019	-0.395
Hormosinella spp.	0.420	0.025	-0.324	-0.142	-0.272	-0.575	-0.475	-0.569
Cystammina argentea	-0.222	-0.278	-0.297	-0.315	-0.212	-0.330	-0.277	-0.263
Miliammina arenacea	0.298	-0.025	-0.225	-0.949	-0.017	**1.352**	**3.796**	0.539
Adercotryma glomerata	**1.293**	0.847	-0.335	-0.129	-0.402	-0.049	-0.700	-0.039
Pseudobolivina antarctica	0.442	0.755	-0.307	-0.222	-0.383	-0.383	-0.536	0.034
Spiroplectammina biformis	-0.261	0.355	0.573	**1.148**	-0.982	-0.937	**3.174**	**-2.129**
Labrospira jeffreysii	-0.255	-0.341	-0.276	-0.400	-0.050	-0.263	-0.134	-0.083
Labrospira sp.	-0.153	-0.362	-0.280	-0.273	-0.173	-0.379	-0.294	-0.289
Eratidus foliaceus	-0.187	-0.179	-0.298	-0.360	-0.216	-0.292	-0.305	-0.234
Paratrochammina bartrami	0.730	-0.639	-0.225	**-1.023**	0.327	0.004	**2.225**	0.948
Recurvoides contortus	-0.198	-0.325	-0.301	-0.280	-0.213	-0.360	-0.293	-0.321
***Portatrochammina* spp.**	**5.534**	-0.008	-0.149	0.514	0.082	0.073	0.031	0.276
Thalmannammina parkerae	-0.099	-0.349	-0.407	-0.251	-0.334	0.579	-0.570	0.432
Alterammina alterans	0.246	0.125	-0.321	-0.145	-0.279	-0.558	-0.455	-0.574
Quinqueloculina sp.	-0.372	-0.349	0.513	-0.404	-0.215	-0.408	-0.207	-0.011
Bolivinellina pseudopunctata	-0.350	-0.403	-0.179	-0.329	**5.715**	0.059	0.426	-0.107
Bolivinellina earlandi	-0.307	-0.325	-0.354	0.036	0.104	-0.234	-0.340	-0.065
Bulimina aculeata	-0.501	0.171	0.097	0.163	-0.601	0.120	-0.072	**5.249**
Angulogerina earlandi	-0.645	0.513	-0.242	-0.381	-0.296	-0.329	-0.028	0.076
Astrononion echolsi	-0.543	-0.277	-0.279	**5.592**	0.539	-0.280	0.207	0.463
Pullenia sphaerica	-0.477	-0.319	-0.238	0.144	-0.173	-0.671	-0.195	0.616
Nonionella iridea	-0.371	-0.201	-0.298	-0.365	-0.164	-0.067	-0.291	-0.182
Rosalina globularis	-0.399	-0.344	-0.242	-0.356	-0.200	-0.266	-0.211	-0.206
Cibicides spp.	-0.403	-0.258	-0.237	-0.367	-0.163	-0.131	-0.260	-0.252
Ioanella tumidula	-0.542	0.167	-0.266	-0.399	-0.242	-0.278	-0.128	-0.062
***Epistominella* spp.**	-0.450	**5.642**	-0.006	-0.177	0.655	0.586	-0.187	-0.007
Stainforthia concava	-0.349	-0.388	-0.332	-0.091	-0.177	-0.103	-0.349	-0.147
Fursenkoina fusiformis	-0.571	-0.545	-0.474	0.426	-0.725	**5.452**	-0.242	-0.856
Cassidulinoides parkerianus	0.316	-0.756	-0.218	-0.416	0.714	0.192	**-1.415**	-0.736
Cassidulinoides porrectus	-0.359	-0.373	-0.283	-0.281	-0.149	-0.304	-0.311	-0.119
Globocassidulina biora	-0.103	-0.156	**5.770**	-0.205	0.009	0.121	-0.134	-0.044
Globocassidulina subglobosa	0.684	-0.283	**1.128**	0.560	0.434	**1.166**	**-1.651**	-0.164

Table 3. Foraminiferal PC loadings. FA values important for particular sites are in bold.

Site	***Portatrochammina* spp. FA**	***Epistominella* spp. FA**	***G. biora* FA**	***A. echolsi* FA**	***B. pseudopunctata* FA**	***F. fusiformis* FA**	***M. arenacea* FA**	***B. aculeata FA***
KG 1	-0.031	-0.059	**0.911**	-0.068	-0.019	-0.021	-0.044	-0.011
KG 7	-0.032	-0.039	**0.945**	-0.049	-0.007	0.003	-0.030	-0.007
KG 13	-0.023	0.248	**0.504**	0.323	**0.687**	0.150	-0.104	-0.005
KG 23	-0.062	-0.089	-0.054	0.024	**0.938**	0.129	0.032	-0.051
KC 1A	-0.048	**0.469**	-0.066	0.106	**0.812**	0.157	0.207	0.031
KC 2B	**0.940**	-0.023	0.117	0.033	0.026	0.108	0.039	0.076
KC 8A	**0.884**	-0.048	-0.042	-0.011	0.036	0.031	0.220	0.118
KC 10	**0.663**	-0.016	-0.052	-0.095	-0.001	0.187	**0.531**	0.122
KC 14	0.387	-0.013	0.118	0.112	0.309	0.168	-0.295	-0.095
KC 21	0.034	-0.057	**0.928**	0.004	0.030	0.099	-0.160	-0.023
KC 28	0.041	0.306	0.018	0.362	**0.410**	**0.727**	0.139	0.034
KC 29	-0.020	-0.070	-0.031	0.156	**0.945**	0.006	0.092	0.011
KC 31	0.295	-0.132	-0.092	-0.010	0.195	0.121	**0.630**	0.254
KC 33	-0.041	-0.049	-0.060	**0.918**	0.122	0.156	0.020	0.046
KC 34	-0.152	-0.070	-0.041	**0.806**	0.193	0.062	0.050	**0.457**
KC 36	-0.002	0.047	-0.039	**0.590**	0.186	**0.733**	-0.015	-0.011
KC 38	0.291	0.009	-0.036	**0.794**	0.292	0.314	-0.028	0.166
KC 45	0.357	0.215	-0.048	0.363	-0.013	**0.424**	-0.112	0.234
KC 46	0.028	-0.019	-0.050	**0.432**	-0.085	**0.792**	0.066	0.343
KC 48	-0.035	-0.013	**0.874**	0.006	-0.039	0.042	0.006	0.183
KC 49	-0.003	0.014	-0.013	0.170	-0.058	0.070	0.018	**0.874**
KC 55	**0.416**	0.011	0.033	0.058	-0.117	-0.031	**0.793**	-0.166
KC 57	-0.021	-0.025	**0.404**	0.014	0.203	**0.810**	0.135	-0.161
KC 60	0.192	0.022	0.189	**0.784**	-0.062	0.225	0.268	-0.201
KC 63	-0.017	0.050	**0.887**	0.086	0.025	0.044	0.147	-0.208
KC 65	0.022	-0.072	-0.028	**0.404**	0.368	0.123	**0.769**	-0.077
KC 6	-0.039	**0.905**	0.001	-0.021	0.018	0.026	-0.012	0.083
KC 9	-0.068	**0.931**	0.003	-0.035	0.092	0.085	-0.038	0.032
KC13	0.281	**0.906**	-0.034	-0.006	0.022	0.006	-0.085	-0.076
KC 15	**0.787**	0.218	-0.074	0.091	-0.106	-0.123	0.087	-0.177
KC 16	**0.919**	0.088	-0.058	0.089	-0.072	-0.055	0.173	-0.032
KC 18	**0.748**	**0.514**	-0.055	0.003	-0.068	0.007	0.058	-0.066
KC 25	**0.673**	**0.700**	-0.074	0.028	-0.013	0.007	-0.057	-0.067
KC 26	0.175	**0.968**	-0.028	0.012	0.017	0.038	-0.010	-0.029

Table 4. *Pearson's* correlation coefficients between various foraminiferal indices. Significant correlation coefficients highlighted in bold.

	Water depth (m)	% calc	p/b ratio	Taxa number	Shan. diversity index	*Portatrochammina spp.* FA	*Epistominella* spp. FA	*G. biora* FA	*A. echolsi* FA	*B. pseudopunctata* FA	*F. fusiformis* FA	*M. arenacea* FA	*B. aculeata* FA
% calc	**-0.45**												
p/b ratio	0.16	0.16											
Taxa_S	**0.57**	-0.03	**0.50**										
Shannon diversity index	**0.61**	-0.21	0.17	**0.79**									
Portatrochammina spp. FA	0.39	**-0.85**	-0.21	0.04	0.17								
Epistominella spp. FA	0.37	-0.07	**0.73**	**0.70**	0.44	0.03							
G. biora FA	**-0.63**	0.41	-0.17	**-0.56**	**-0.60**	-0.34	-0.26						
A. echolsi FA	0.02	0.28	-0.20	0.08	0.34	-0.27	-0.28	-0.26					
B. pseudopunctata FA	-0.22	0.45	-0.12	0.04	-0.06	-0.39	-0.12	-0.15	0.11				
F. fusiformis FA	-0.10	0.30	-0.09	0.04	0.26	-0.28	-0.17	-0.12	0.38	0.12			
M. arenacea FA	0.12	**-0.55**	-0.19	-0.27	-0.03	0.15	-0.28	-0.25	-0.03	-0.03	-0.06		
B. aculeata FA	0.15	0.15	0.01	-0.09	-0.08	-0.17	-0.17	-0.20	0.18	-0.09	0.09	-0.09	
Rhabdammina spp.	0.38	-0.31	0.28	**0.54**	0.45	0.26	**0.60**	-0.21	-0.01	-0.33	-0.23	-0.10	-0.30
Psammosphaera fusca	-0.35	0.13	-0.13	-0.38	-0.43	-0.10	-0.19	**0.57**	-0.26	-0.16	-0.19	-0.18	-0.09
Lagenammina arenulata	0.09	-0.04	-0.11	-0.07	0.14	-0.18	-0.27	-0.27	0.34	0.12	0.08	0.44	0.23
Reophax subdentaliniformis	-0.12	-0.10	-0.10	-0.17	-0.02	-0.08	-0.16	0.26	0.02	-0.20	-0.05	0.12	0.13
Reophax scorpiurus	0.15	0.09	0.03	0.19	0.18	-0.17	-0.08	-0.30	0.45	-0.10	0.06	-0.06	0.45
Reophax cf. *R. spiculifer*	**0.67**	-0.44	0.02	**0.52**	0.47	**0.50**	0.37	-0.24	-0.20	-0.29	-0.35	-0.10	-0.28
Nodulina cf. *N. dentaliniformis*	-0.11	-0.14	-0.15	0.09	0.06	0.04	-0.19	-0.11	0.10	0.11	-0.07	0.28	-0.27
Hormosinella spp.	**0.65**	-0.47	0.04	**0.53**	0.49	**0.56**	0.43	-0.25	-0.23	-0.29	-0.36	-0.13	-0.28
Cystammina argentea	**0.63**	-0.44	0.04	**0.58**	0.48	**0.50**	0.47	-0.25	-0.22	-0.29	-0.34	-0.12	-0.27
Miliammina arenacea	0.03	**-0.54**	-0.19	-0.24	-0.02	0.27	-0.20	-0.28	-0.14	-0.08	0.13	**0.77**	0.05
Adercotryma glomerata	0.46	**-0.56**	0.01	0.48	0.47	**0.62**	**0.50**	-0.37	-0.24	-0.33	-0.16	-0.13	-0.08
Pseudobolivina antarctica	0.49	-0.38	0.18	0.60	0.45	0.39	**0.60**	-0.30	-0.23	-0.33	-0.26	-0.21	-0.01
Spiroplectammina biformis	0.08	-0.34	-0.11	-0.11	0.10	0.06	-0.06	0.08	0.00	-0.23	-0.19	**0.58**	-0.41
Labrospira jeffreysii	-0.13	-0.24	0.03	-0.09	0.03	0.32	-0.03	-0.23	-0.18	0.06	-0.09	0.15	0.05
Labrospira sp.	0.40	-0.33	-0.10	0.41	0.37	0.45	0.04	-0.14	-0.11	-0.09	-0.29	-0.03	-0.22
Eratidus foliaceus	0.39	-0.31	0.02	0.33	0.31	0.37	0.37	-0.17	-0.18	-0.20	-0.19	-0.10	-0.16
Paratrochammina bartrami	0.12	**-0.55**	-0.15	-0.36	-0.26	0.43	-0.26	-0.24	-0.21	-0.05	-0.11	**0.55**	0.10
Recurvoides contortus	**0.60**	-0.35	-0.06	0.34	0.37	0.42	0.15	-0.17	-0.12	-0.22	-0.26	-0.05	-0.23
Portatrochammina spp.	0.23	**-0.75**	-0.17	-0.16	-0.09	**0.87**	-0.09	-0.35	-0.21	-0.28	-0.18	0.21	-0.01
Thalmannammina parkerae	0.06	-0.04	-0.10	0.03	0.21	0.00	-0.09	-0.19	0.20	-0.03	0.32	-0.08	0.26
Alterammina alterans	**0.64**	-0.39	0.10	0.49	0.44	0.42	**0.50**	-0.23	-0.22	-0.27	-0.32	-0.16	-0.27
Quinqueloculina sp.	-0.47	0.26	-0.10	-0.39	**-0.52**	-0.19	-0.17	**0.57**	-0.22	-0.15	-0.18	-0.15	-0.07
Bolivinellina pseudopunctata	-0.12	0.38	-0.17	0.07	-0.10	-0.34	-0.20	-0.16	0.04	**0.92**	0.04	0.02	-0.08
Bolivinellina earlandi	0.10	0.25	-0.18	0.18	0.26	-0.15	-0.13	-0.34	**0.55**	0.43	0.19	-0.10	0.16
Bulimina aculeata	0.25	0.19	0.04	0.02	0.03	-0.24	-0.08	-0.12	0.15	-0.18	0.06	-0.12	**0.88**
Angulogerina earlandi	0.10	0.13	**0.83**	0.39	0.15	-0.18	**0.59**	-0.12	-0.18	-0.09	-0.13	-0.14	0.00
Astrononion echolsi	-0.03	0.36	-0.17	0.06	0.21	-0.37	-0.31	-0.28	**0.92**	0.27	0.28	-0.02	0.26
Pullenia sphaerica	0.23	0.19	-0.07	0.00	0.05	-0.23	-0.15	-0.12	0.36	-0.02	-0.09	-0.06	**0.56**
Nonionella iridea	0.16	0.19	**0.62**	0.48	0.37	-0.10	**0.61**	-0.20	-0.07	0.11	0.29	-0.28	-0.10
Rosalina globularis	-0.08	0.18	0.02	-0.15	-0.11	-0.22	-0.04	0.44	-0.08	-0.03	0.03	0.00	-0.15
Cibicides spp.	-0.11	0.33	**0.53**	0.17	0.04	-0.25	0.23	0.07	0.03	-0.01	0.13	-0.20	-0.22
Ioanella tumidula	0.12	0.13	**0.98**	0.48	0.13	-0.20	**0.74**	-0.14	-0.24	-0.12	-0.16	-0.18	-0.03
Epistominella spp.	0.22	0.12	**0.86**	**0.64**	0.35	-0.16	**0.93**	-0.22	-0.22	0.02	-0.08	-0.29	-0.14
Stainforthia concava	0.02	0.27	-0.01	0.07	0.15	-0.15	-0.11	-0.18	**0.56**	0.10	0.39	-0.15	0.18
Fursenkoina fusiformis	-0.02	0.32	-0.15	0.10	0.28	-0.30	-0.26	-0.13	0.46	0.09	**0.93**	-0.04	0.05
Cassidulinoides parkerianus	-0.24	0.22	-0.11	0.00	0.04	-0.01	-0.15	-0.02	-0.04	0.25	0.07	-0.28	-0.18

Cassidulinoides porrectus	-0.04	0.23	-0.11	0.00	0.07	-0.10	-0.18	-0.09	0.23	0.15	-0.06	-0.24	0.16
Globocassidulina biora	**-0.61**	0.41	-0.17	**-0.56**	**-0.66**	-0.32	-0.26	**0.96**	-0.28	-0.17	-0.15	-0.25	-0.17
Globocassidulina subglobosa	-0.40	0.33	-0.16	-0.27	-0.12	-0.10	-0.17	0.47	0.11	0.03	0.22	-0.42	-0.10